Composite 133 lpi at 45 degrees

EARTH SCIENCES
RESEARCH JOURNAL

Earth Sci. Res. J. Vol. 12, No. 2 (December 2008): 235-264

MULTIDISCIPLINARY APPROACH TO STUDY MIGMATITES: ORIGIN AND TECTONIC HISTORY OF THE NASON RIDGE MIGMATITIC GNEISS, WENATCHEE BLOCK, CASCADES CRYSTALLINE CORE, WA, USA

Carlos A. Zuluaga C.[1] ***and Harold H. Stowell***[2]

[1] *Departament of Geosciences, Universidad Nacional de Colombia.*

[2] *Department of Geological Sciences, University of Alabama, Tuscaloosa, AL 35487.*

ABSTRACT

The Nason Ridge Migmatitic Gneiss of the Cascades Core is a migmatitic unit comprising concordant pelitic schist and gneiss, amphibolite, and tonalite gneiss, and cross cutting tonalite, quartz-rich granitoid, and pegmatite. There are several generations of ‘igneous’ lithologies (leucosomes = tonalite, quartz-rich granitoid, and pegmatite) some of which are concordant; others clearly crosscut the strongly deformed host rocks. The host rocks are interpreted to be Chiwaukum Schist with metasedimentary (pelitic schist and some gneiss) and metavolcanic (amphibolites) origins. Metamorphic fabric in the Nason Ridge Migmatitic Gneiss is characterized by preferred orientation of platy minerals (continuous schistosity), compositional layering, mineral lineations (elongate grains and grain aggregates), and non-coaxial deformational features (asymmetric augen, grain offsets, rotated porphyroblasts, etc.). Compositional layering is characterized by quartz-plagioclase lenses and patches (mm to cm scale) and by large variations in biotite content. This composite fabric is faulted and folded by mesoscopic structures. The most strongly foliated leucosomes (gneissic tonalites) are generally concordant with the regional trend of foliation, while weakly foliated leucosomes (tonalites) and pegmatite veins crosscut host rock and tonalite gneisses. Thin melanosome layers (biotiteand amphibole schist) are developed locally around quartz – plagioclase lenses and patches. Metamorphism in the Nason Ridge Migmatitic Gneiss and the nearby Chiwaukum Schist likely peaked after intrusion of the Mt. Stuart Batholith ca. 91-94 Ma. Peak temperatures and pressures for the Nason Ridge Migmatitic Gneiss in the Wenatchee Ridge and Pacific Crest areas were 650 - 720 °C and 6 - 9 kbar with a pressure increase of ≤ 2.0 kbar during metamorphism.

Thermodynamic modeling indicates that hydrous partial melting would begin at ca. 660 °C and is relatively pressure independent. Field and petrographic observations, mineral chemistry and thermobarometry, and bulk rock chemistry and thermodynamic modeling of phase equilibria (pseudosections) applied to the Nason Ridge

Manuscript received: June 10th, 2008.
Accepted for publication: November 11th, 2008.

FEBRERO 20-GEOCIENCIAS-VOL 12-2 ULTIMA VERSION.prn
D:\GEOCIENCIAS V-12-2-DIC 2008\GEOCIENCIAS-VOL 12-2 DIC.vp
viernes, 20 de febrero de 2009 13:08:56

Composite 133 lpi at 45 degrees

Migmatitic Gneiss indicate that at least some of the leucosome bodies were derived by local partial melting. The clearly intrusive character and the sharp contacts between some tonalite leucosome bodies and host rock support an externally derived origin for these tonalite melts. However, some of these bodies may have originated from partial melting of the host Chiwaukum Schist and traveled a short distance before crystallization, or have been modified by deformation so as to obscure textural evidence for local derivation. Results are compatible with derivation of leucosome rocks in the Nason Ridge Migmatitic Gneiss from two non-exclusive processes: partial melting of the host rock and intrusion of externally derived tonalite melts.

Key words: Migmatites, partial melting, Cascades Core, thermodynamic modeling, Nason Ridge Migmatitic Gneiss.

RESUMEN

La unidad "Nason Ridge Migmatitic Gneiss" del "Cascades Core" (NW de los Estados Unidos) es una unidad migmatítica que comprende esquisto y gneis pelítico, anfibolita, gneis tonalítico y tonalita concordantes y tonalita, granitoide cuarzoso y pegmatita discordantes. Hay varias generaciones de litologías ígneas (leucosomas = tonalita, granitoide cuarzoso, y pegmatita) algunos de las cuales son concordantes; otras claramente cortan la roca caja que está fuertemente deformada. La roca caja se interpreta ser la unidad "Chiwaukum Schist" que es una unidad metasedimentaria (esquisto pelítico y algunos gneises) y metavolcánica (anfibolitas). La fábrica metamórfica en el Nason Ridge Migmatitic Gneiss está caracterizada por la orientación preferencial de minerales micáceos (esquistosidad continua), bandeamiento composicional, lineación mineral (granos y agregados elongados), y rasgos de deformación no-coaxial (augen asimétrico, granos cortados y desplazados, porfiroblastos rotados, etc.). El bandeamiento composicional está caracterizado por lentes y parches (a escala milimétrica y centimétrica) de cuarzo y plagioclasa y por variaciones grandes en contenido de biotita. Esta fabrica compuesta esta fallada y plegada por estructuras mesoscópicas. Los leucosomas con foliación más pronunciada (tonalitas gnéisicas) son generalmente concordantes con la tendencia regional de la foliación, mientras que los leucosomas débilmente foliados (tonalitas) y las venas de pegmatita cortan la roca caja y el gneis tonalítico. Capas delgadas de melanosoma (esquisto de biotita y de anfíbol) se desarrollan localmente alrededor de los lentes y parches de cuarzo y plagioclasa. El pico del metamorfismo en el Nason Ridge Migmatitic Gneiss y en el Chiwaukum Schist probablemente ocurrió después de la intrusión del batolito "Mt. Stuart" (ca. 91-94 Ma.). Las temperaturas y las presiones del pico del metamorfismo en las regiones de "Wenatchee Ridge" y del "Pacific Crest" fueron 650-720 °C y 6-9 kbar con un aumento de presión de ≤ 2.0 kbar durante el metamorfismo.

El modelamiento termodinámico indica que la fusión parcial acuosa comenzaría aproximadamente a 660 °C y que esta temperatura es relativamente independiente de la presión. Observaciones de campo y petrográficas, química mineral y estimaciones termobarométricas, y la química de roca total y modelos termodinámicos de equilibrios de fases (pseudosecciones) aplicados al Nason Ridge Migmatitic Gneiss indican que por lo menos algunos de los cuerpos de leucosoma fueron derivados por fusión parcial local. El carácter claramente intrusivo y los contactos abruptos entre algunos cuerpos de tonalita y la roca caja apoyan un origen externo para estos fundidos de tonalita. Sin embargo, algunos de estos cuerpos pudieron haberse originado por fusión parcial del Chiwaukum Schist y haber viajado una distancia corta antes de la cristalización, o pueden haber sido modificados por deformación y así oscurecer la evidencia textural que indicaría derivación local. Los resultados mostrados aquí son compatibles con derivación de leucosomas en el Nason Ridge Migmatitic Gneiss a partir de dos procesos no exclusivos: fusión parcial de la roca caja e intrusión de fundidos tonaliticos derivados externamente.

FEBRERO 20-GEOCIENCIAS-VOL 12-2 ULTIMA VERSION.prn
D:\GEOCIENCIAS V-12-2-DIC 2008\GEOCIENCIAS-VOL 12-2 DIC.vp
viernes, 20 de febrero de 2009 13:08:56

Composite 133 lpi at 45 degrees

Palabras clave: Migmatitas, fusión parcial, Cascades Core, modelos termodinámicos, Nason Ridge Migmatitic Gneiss

Introduction

This paper presents a multidisciplinary methodology to fully characterize a migmatitic unit: the Nason Ridge Migmatitic Gneiss (NRMG). The NRMG is one of three metamorphic culminations in the Cascades magmatic arc of the Cascades Crystalline Core (Cascades Core). The origin and metamorphic history of the NRMG constrains the deep crustal evolution of the magmatic arc; however, its origin is enigmatic and few data are available to constrain interpretations. The unit has been interpreted as one of the most deeply exhumed parts of the Nason terrane (Brown and Walker, 1993; Miller and Paterson, 2001). Multiple techniques are used to elucidate the origin of the NRMG migmatites exposed in the Wenatchee Ridge area (Figure 1). Techniques include: petrographic analysis, thermobarometric calculations and *P-T* pseudosections. Pseudosections are used to construct quantitative *P-T* paths for metamorphism and to predict conditions for partial melting. Thermobarometry and *P-T* pseudosections indicate that garnet grew over temperatures from 550 to 700 °C with a negligible to moderate pressure increase of ≤ 2.0 kbar. *P-T* estimates from thermobarometry and pseudosection modeling support petrographic interpretations that partial melting produced leucosome quartz – plagioclase lenses in the NRMG.

Methods

Textural analysis

Changes that rocks experience during metamorphism may be recorded in the mineralogy and texture. Partial melting of a rock suite generally produces identifiable petrographic characteristics that yield infor- mation about metamorphism and tectonic events. Macroscopic textures are the first and the simplest criteria that can be used to identify if a suite of rocks had been formed by partial melting. The presence of melanosome layers or patches (e.g., biotite selvages) provides the best evidence of local melt formation, and the presence of leucosome (rich in non-ferromagnesian minerals – generally quartz and feldspar), where the melt collected (Sawyer, 1999). Thin section analysis of textures and mineral assemblages was used to identify mineral assemblages that may have undergone melting and the potential melt forming reactions (e.g., Sawyer, 1999) and/or microscopic textures generally linked with partial melting processes (Sawyer, 1999; Mehnert *et al.,* 1973; Ashworth and McLellan, 1985). These microscopic textures include: 1) thin films of plagioclase, quartz, and K-feldspar along grain boundaries (crystallized melt), and 2) melt-solid reaction textures. Macroscopic features, assigned to partial melting, are readily identified in some mesosome rocks from the Nason Ridge Migmatitic Gneiss. On the other hand, microscopic features related to partial melting cannot be identified in Nason Ridge Migmatitic Gneiss rocks; likely because of extensive deformation. However, mineral parageneses identified in thin sections are important for constraining thermodynamic models.

Bulk rock chemistry

Whole-rock compositions were determined by X-ray fluorescence from fused glass discs (samples were analyzed by Activation Laboratories, Ltd. and at The University of Alabama analytical facilities). One sample (00NC9d) was analyzed in both laboratories for interlaboratory comparison. Bulk rock samples were ground on a diamond embedded lap to remove surfaces that were obviously weathered or cut by the rock saw. Approximately 30 g of resulting 'fresh' sample was washed, and rinsed in acetone and 2M HCl before jaw crushing and grinding to a powder in a steel ring-and-puck mill. Samples prepared and analyzed at The University of Alabama were dried in two steps (120 ºC followed by ca. 1000 ºC), mixed with flux (lithium tetraborate 67% - lithium metaborate 33%) in

FEBRERO 20-GEOCIENCIAS-VOL 12-2 ULTIMA VERSION.prn
D:\GEOCIENCIAS V-12-2-DIC 2008\GEOCIENCIAS-VOL 12-2 DIC.vp
viernes, 20 de febrero de 2009 13:08:56

Composite 133 lpi at 45 degrees

a 1:9 proportion (sample/flux), and combined with a drop of lithium bromide non-wetting agent. This mix was fused in a platinum-gold crucible using a gas burner, and cast into a 32 mm diameter disc using a platinum-gold mold. Glass discs were analyzed with The University of Alabama Phillips PW2400 X-ray fluorescence spectrometer equipped with a Rh X-ray tube. Calibration was based on 15 to 20 certified rock standards per element.

Mineral chemistry

Quantitative mineral analyses and X-ray maps were collected with the JEOL 8600 electron probe microanalyzer at The University of Alabama using wavelength dispersion spectrometry. Major element analyses were collected with a 1 to 20 μm diameter beam at a current of 20 nA under a 15 kV accelerating potential. Raw counts from characteristic X-ray peaks were converted to weight percent oxides by comparison to natural mineral and synthetic standards, using the CitZAF correction technique of Armstrong (1984). Count times ranged from 30 to 45 seconds. Operating conditions for collection of X-ray maps were 15 kV accelerating potential, 75 to 300 nA beam current, and a 1 μm beam. Count times ranged from 50 to 100 ms pixel.

Thermodynamic modeling and P-T paths for metamorphism

Several methods have been used for constructing *P-T* paths for rocks (Spear and Selverstone, 1983; Spear, 1988; St-Onge, 1987; Stowell et al, 2001, Tinkham, 2002). The *P-T* paths constructed here follow the methods of Vance and Mahar (1998), Stowell et al. (2001), and Stowell and Tinkham (2003). Garnet rim thermobarometry was used to estimate *P-T* at peak

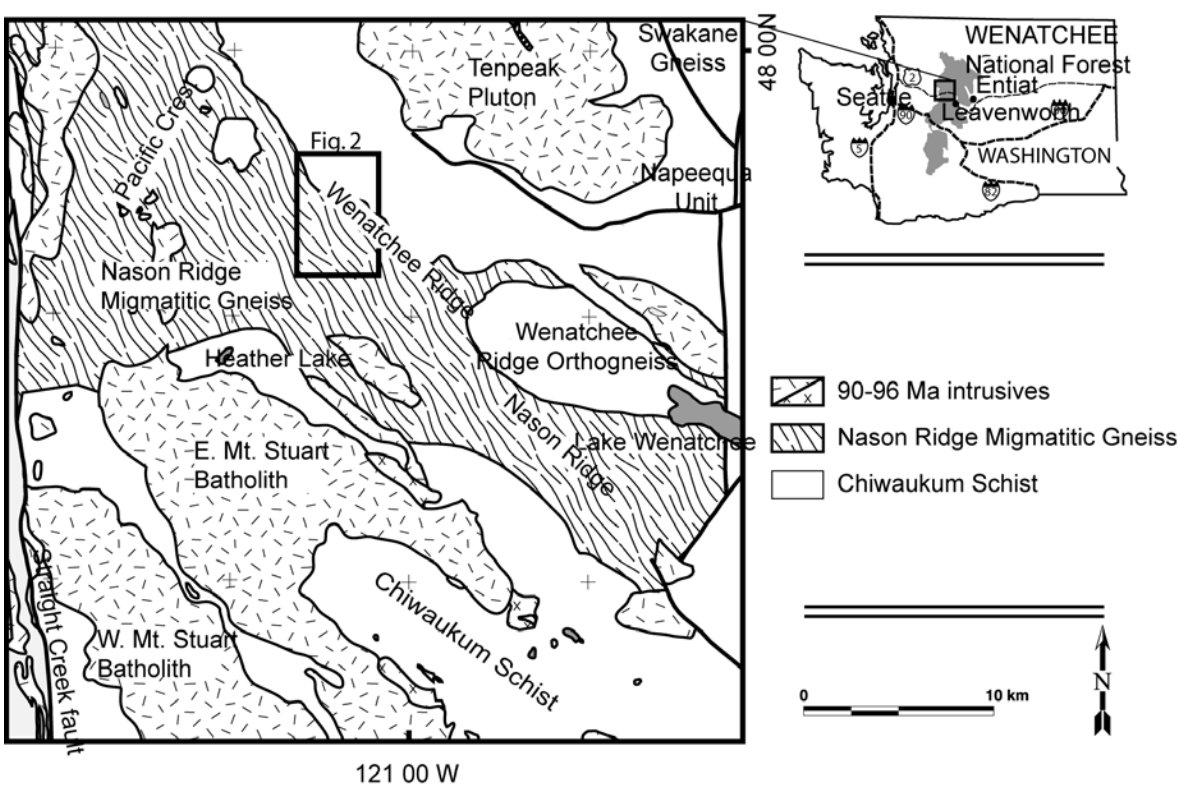

Figure 1. Generalized geologic map of the Wenatchee block in the Cascades Core, WA. Note the distribution of the main geologic units in the Nason terrane: Chiwaukum Schist, Nason Ridge Migmatitic Gneiss, and Mt. Stuart Batholith.

FEBRERO 20-GEOCIENCIAS-VOL 12-2 ULTIMA VERSION.prn
D:\GEOCIENCIAS V-12-2-DIC 2008\GEOCIENCIAS-VOL 12-2 DIC.vp
viernes, 20 de febrero de 2009 13:08:57

Composite 133 lpi at 45 degrees

metamorphic conditions with the average *P-T* routine of THERMOCALC (v. 3.21; Powell and Holland, 1988; Powell *et al.,* 1998) using externally calculated activities. Activities were calculated using pressures and temperatures close to the estimated *P-T* conditions, then input in THERMOCALC for linearization of reactions or for average *P-T* calculation (Powell and Holland, 1994). Activities and *P-T* estimates were refined by iteration until calculation and estimated temperatures and pressures differ in less than 5 ºC and 0.1 kbar, respectively. Estimates for peak pressures and temperatures were further refined with pseudosection fields following the technique presented in Zuluaga et al. (2005). Garnet core compositions were plotted as the compositional variables spessartine, grossular, and iron number (Fe# = Fe/Fe+Mg) in *P-T* pseudosections (isopleths). Ideally, the three isopleths intersect at a single point, but frequently this is not the case because of the uncertainties in analytical data and in model calculations. However, the area bounded by isopleth intersections provides an estimate for initial garnet growth *P-T* conditions. Initial garnet growth *P-T* estimates were integrated with garnet rim thermobarometry to provide a simplified finite *P-T* path for garnet growth. Pseudosections were constructed using the computer program THERMOCALC and the thermodynamic database of Holland and Powell (1998) with the silicate melts model extension (Holland and Powell, 2001; White *et al.*, 2001; th pdata files created February 13, 2002). All thermodynamic models used the nine-component oxide system: MnO, Na_2O, CaO, K_2O, FeO, MgO, Al_2O_3, SiO_2, and H_2O (MnNCKFMASH) because this is the minimum system needed to realistically predict mineral stability for garnet-bearing pelites (Tinkham *et al.*, 2001). Except for the melt phase, activity models used here are the same as those used and discussed in Tinkham *et al.,* (2001). Melt activity models are the same as those presented in Holland and Powell (2001) and White et al (2001).

Regional geology

The Cascades Core of the North Cascades and the Coast Plutonic Complex to the north represent the roots of a Mesozoic to early Tertiary magmatic arc. Mesozoic metamorphic rocks and Cretaceous to Tertiary plutons crop out in the Cascades Core in a mosaic of amalgamated terranes. The overall tectonic history of the Cascades Core has been discussed in several publications (e.g., Brown *et al.,* 1994; Evans and Davidson; 1999; Miller *et al.,* 1994; Tabor *et al.,* 1993). The post metamorphic high angle Entiat fault divides the Cascades Core into two tectonic blocks with different thermal histories, the Wenatchee and Chelan Blocks (Miller *et al.,* 1994; Miller and Paterson, 2001; Haugerud *et al.,* 1991). This paper focuses on the Wenatchee Block and does not discuss the Chelan Block. The most prominent metamorphic rock units in the Wenatchee Block are part of the Nason terrane. The Nason terrane consists of dominantly metasedimentary Chiwaukum Schist and the migmatitic Nason Ridge Migmatitic Gneiss.

The earliest metamorphic event in the Chiwaukum Schist was a poorly understood pre-Mount Stuart amphibolite facies regional metamorphic event (M_1^R)(e.g., Evans and Davidson, 1999). M_1^R mineral assemblages were overprinted by minerals that grew during Buchan style dynamic contact metamorphism associated with the Mount Stuart Batholith (M_2^C)(Evans and Berti, 1986) and other Late Cretaceous plutons. Late Cretaceous contact metamorphism was followed by Barrovian style regional metamorphism (M_3^R)(Evans and Berti, 1986; Evans and Davidson, 1999; Tinkham, 2002). Rocks adjacent to Late Cretaceous plutons typically contain M_2^C and M_3^R mineral assemblages: for example, andalusite + cordierite ± garnet are typical of M_2^C, and staurolite + kyanite + garnet are typical of M_3^R (Evans and Berti, 1986; Tinkham, 2002). Chiwaukum Schist dominantly comprises metasedimentary rocks (aluminous biotite-rich schists) and lesser amounts of metavolcanic rocks (amphibolite) with penetrative foliation, predominantly continuous schistosity, and lineation defined by mineral alignment. The Nason Ridge Migmatitic Gneiss contains biotite-rich and/or muscovite-rich schist, amphibolite, quartzite, and minor calc-silicate layers, and layers, lenses, patches, and veins of granitoid rocks yielding a migmatitic texture (Van Diver, 1967).

FEBRERO 20-GEOCIENCIAS-VOL 12-2 ULTIMA VERSION.prn
D:\GEOCIENCIAS V-12-2-DIC 2008\GEOCIENCIAS-VOL 12-2 DIC.vp
viernes, 20 de febrero de 2009 13:08:57

Composite 133 lpi at 45 degrees

Thermobarometry in the Nason terrane yields temperatures of 500-700 °C and systematic trends in pressure increasing from ca. 3 kbar, in the south to ca. 9 kbar in the northeast (Brown and Walker, 1993; Tinkham, 2002). Several tectonic models have been developed to explain the metamorphic and structural features of the Cascades Core. These models can be grouped into two types: (1) orogen normal contraction, produced by bulk-shortening in a pure shear setting (Whitney and McGroder, 1989; McGroder, 1991; Whitney, 1992a; Whitney *et al.*, 1999; Paterson *et al.,* 2004; Stowell *et al.*, 2007) and (2) orogen parallel strike slip in a simple shear setting (Brown and Talbot, 1989; Brown and Walker, 1993; Brown *et al.*, 1994; Walker and Brown, 1991).

Thermal relaxation signature characterized by a fairly rapid pressure increase followed by temperature increase during garnet growth supports the orogen normal contraction model with loading by a tapered thrust sheet (Stowell *et al.*, 2007). Late Cretaceous thrusting is preserved at the southern margin of the Wenatchee Block, where the Ingalls Ophiolite Complex was thrust over the Chiwaukum Schist (Windy Pass Thrust). Other evidence for thrusting is observed on the western border of the Cascades Core where an assemblage of oceanic sedimentary and volcanic rocks, were thrust onto the magmatic arc along a complex array of faults known as the Northwest Cascades System. Metamorphic stretching lineations throughout the Cascades Core show a horizontal NW-SE preferred orientation and shear sense features indicate non-coaxial right-lateral motion (Brown and Talbot, 1989). Evidence for non-coaxial deformation includes asymmetric augen and porphyroclasts, rotated (snowball) porphyroclasts, S-C fabrics, and grain offsets. Strain partitioned folding might have been the cause for the lack of structural evidence for thrusting and steepening of paleobarimetric gradients (Stowell *et al.*, 2007).

Textural and compositional description of the Nason Ridge Migmatitic Gneiss

Rosenberg (1961) and Van Diver (1967) reported the first detailed studies of the Nason Ridge Migmatitic Gneiss. Rosenberg (1961) subdivided the Chiwaukum Schist into the "Whittier Peak unit" and "Poe Mountain unit", the last being the equivalent of the Nason Ridge Migmatitic Gneiss. Van Diver (1967) produced a detailed petrographic study of these rocks in the Wenatchee Ridge area. He interpreted that this unit formed by granitization of Chiwaukum Schist following a migmatization front that focused around the Wenatchee Ridge Orthogneiss. Magloughlin (1986, 1989, and 1993) determined metamorphic conditions from thermobarometric calculations and described pseudotachylites and other cataclastic rocks in the Chiwaukum Schist and Nason Ridge Migmatitic Gneiss on Wenatchee Ridge. Taylor (1994) and Miller and Paterson (2001) presented results from structural studies on the Chiwaukum Schist, which displays a strong composite schistosity resulting from transposed cycles of folding. Tinkham (2002) and Stowell and Tinkham (2003), reported garnet Sm-Nd geochronology and *P-T-t* paths for rocks at the western end of the Nason Ridge Migmatitic Gneiss near Heather Lake (Figure 1). These studies indicate that garnet grew at ca. 86 – 88 Ma (after Mt. Stuart emplacement ca. 93.5 Ma) during the latter stages of crustal loading recording 0 to ≤ 2 kbar of pressure increase along the heating path.

The Nason Ridge Migmatitic Gneiss is an elongate northwest to southeast oriented body within the Chiwaukum Schist (Figure 1). Gradational contacts with the adjacent Chiwaukum Schist have been used to infer that the Nason Ridge Migmatitic Gneiss originated from a Chiwaukum Schist protholith. In the Wenatchee Ridge area, Nason Ridge Migmatitic Gneiss is composed mainly of schist and gneiss with lesser volumes of tonalites, pegmatites and amphibolites. The rocks are classified into leucosomes, mesosomes, and melanosomes; following that scheme, textures and mineralogy for each lithology are discussed below. Figures 2 and 3 portray the lithological and structural features of the Nason Ridge Migmatitic Gneiss and sample localities discussed here along Wenatchee Ridge and the Pacific Crest. Table 1 summarizes the most important petrographic features of samples described in the text.

FEBRERO 20-GEOCIENCIAS-VOL 12-2 ULTIMA VERSION.prn
D:\GEOCIENCIAS V-12-2-DIC 2008\GEOCIENCIAS-VOL 12-2 DIC.vp
viernes, 20 de febrero de 2009 13:08:57

Composite 133 lpi at 45 degrees

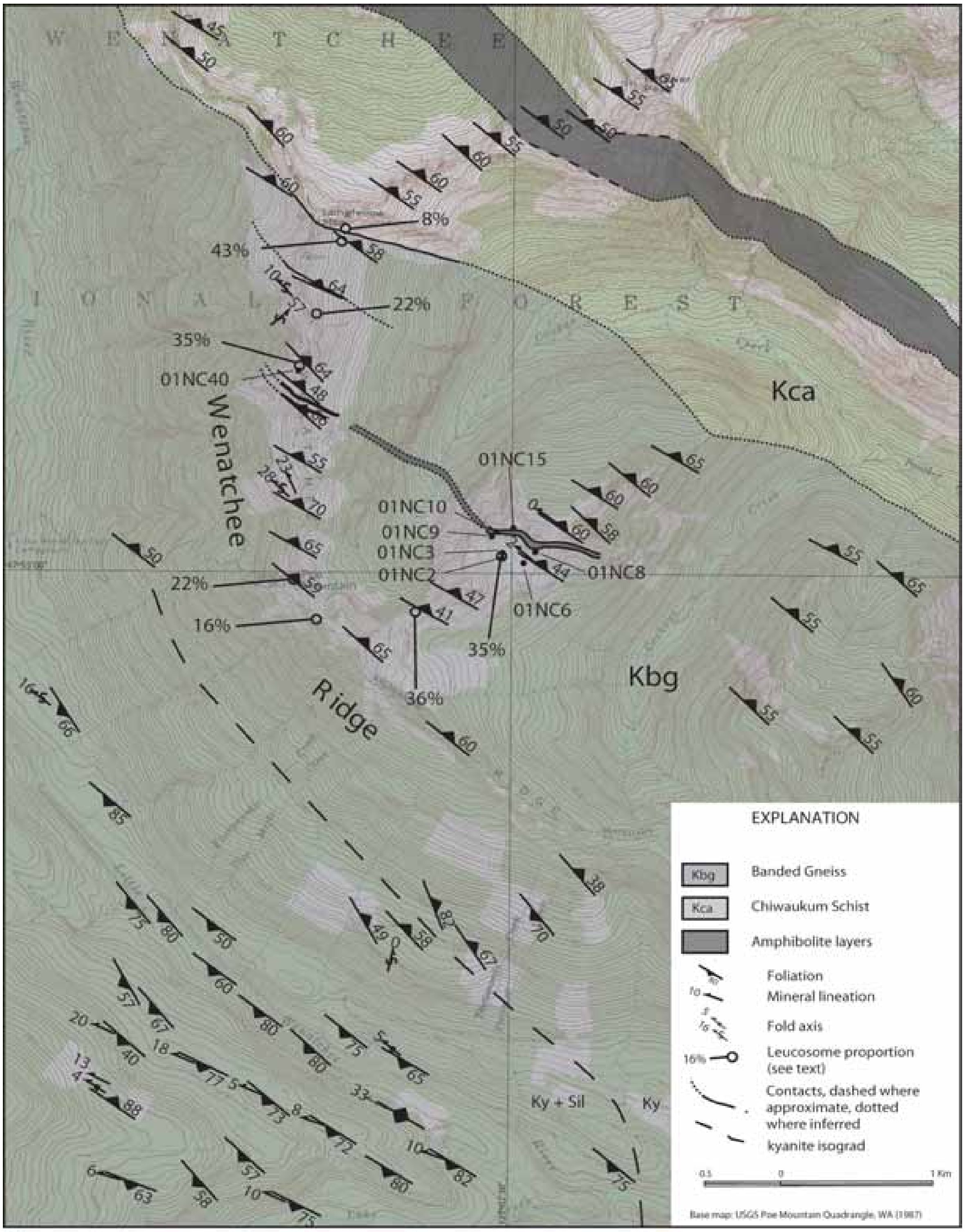

Figure 2. Geologic map of the Wenatchee Ridge area, Cascades Core, WA. Location provided on Fig. 1. Data to the northeast and to the southwest from Van Diver (1967).

FEBRERO 20-GEOCIENCIAS-VOL 12-2 ULTIMA VERSION.prn
D:\GEOCIENCIAS V-12-2-DIC 2008\GEOCIENCIAS-VOL 12-2 DIC.vp
viernes, 20 de febrero de 2009 13:09:01

Composite 133 lpi at 45 degrees

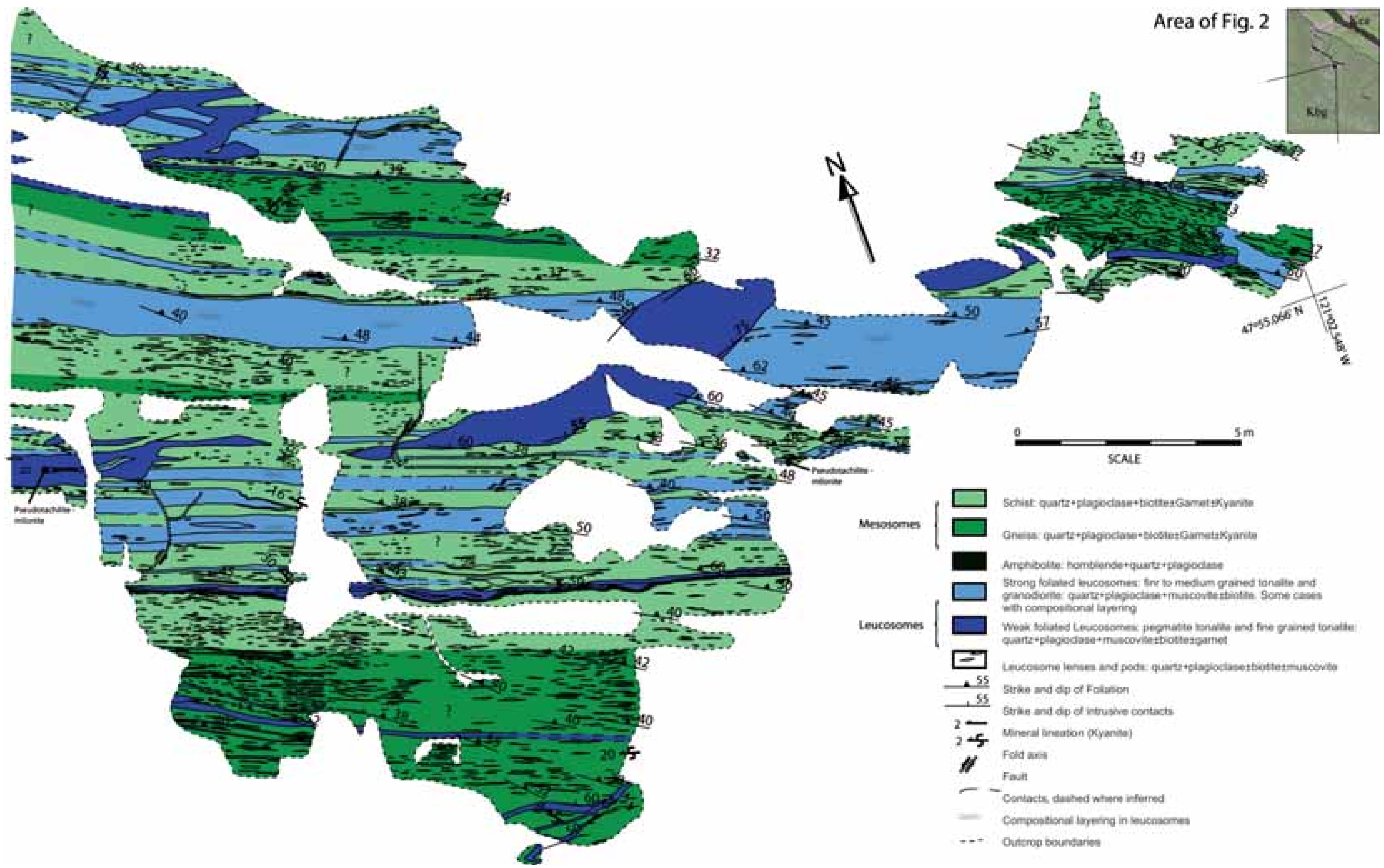

Figure 3. Outcrop map of Nason Ridge Migmatitic Gneiss east of Poe Mountain, Wenatchee Ridge, WA. This map illustrates contact relations and distribution of mesosome and leucosome lithologies. Note also structures at centimeter to meter scale.

FEBRERO 20-GEOCIENCIAS-VOL 12-2 ULTIMA VERSION.prn
D:\GEOCIENCIAS V-12-2-DIC 2008\GEOCIENCIAS-VOL 12-2 DIC.vp
viernes, 20 de febrero de 2009 13:09:04

Composite 133 lpi at 45 degrees

Table 1. Petrography of Nason Ridge Migmatitic Gneiss lithologies, Cascades Core, WA.

Samples	Qtz	Pl	Kfs	Ms	Bt	Hbl	Cam	Grt	Ky	Sil	Tur	Ep	Accessories	Name; textures
Leucosomes														
01NC2a	35	30	10	20	5	-	-	-	-	-	-	-	Grt, Czo, Zrn, Rt	Granodiorite; FG-SF, IZ-MI, D
01NC2b	45	40	-	15	-	-	-	-	-	-	-	-	Rt.	Pegmatite tonalite; WF, D
01NC2c	70	30		Tr	Tr	-	-	Tr	-	-	-	-		Qtz-Pl lens; Granoblastic
01NC3b	30	35	-	35	-	-	-	-	-	-	-	-	Ep, Ap, Zrn, Rt, Grt	Tonalite; MG-WF, MI, D
01NC8a	40	35	-	15	5	-	-	-	-	-	-	-	Ap, Zrn, Ep	Tonalite; SF, MI, C
01NC8c	23	75	-	-	1	-	-	-	-	-	-	-	Ms, Spn, Ap, Zrn, Chl	Pegmatite tonalite; CG-WF, IZ, C
01NC9a	35	37	15	-	-	-	-	-	-	-	-	-	Ep, Ap, Zrn.	Granodiorite; FG-MG-SF, MI, PI, D
1 01NC9b	40	35	15	10	-	-	-	-	-	-	-	-	Bt, Ap, Zrn, Ep, Czo, Op	Granodiorite; MG-SF, MI, D
01NC15c	45	35	-	15	5	-	-	-	-	-	-	-	Ep, Ap, Chl	Tonalite; FG-WF, IZ, D
01NC15a	60	20	-	20	-	-	-	-	-	-	-	-	Grt, Ap, Zrn.	Pegmatite Qtz-granitoid; WF, MI,D
Mesosomes														
01NC2c	55	15	-	2	20	-	-	5	2	-	-	-	Rt, Zrn, Ap	Grt-Ky-Tur gneiss; Lep-Gran
01NC3a	55	20	-	Tr	25	-	-	Tr	-	-	-	-	Ap, Zrn, Rt	Bt-Grt schist; Lepidoblastic
01NC6	50	20	-	3	15	-	-	5	5	-	Tr	Tr	Ap, Zrn, Rt(2%), Czo	Grt-Ky schist; Lepidoblastic
01NC8d	7	8	-	Tr	-	80	-	2	-	-	-	-	Spn(3%), Ap, Rt, Chl	Grt amphibolite; Lepidoblastic
01NC9c	40	33	-	1	25	-	-	1	-	-	-	Tr	Ap, Rt, Zrn	Grt schist; Lepidoblastic
01NC9d	40	30	-	2	17	-	-	5	3	-	Tr	-	Chl (3%), Rt, Zrn, Ap	Grt-Ky schist; Lep-Gran

FEBRERO 20-GEOCIENCIAS-VOL 12-2 ULTIMA VERSION.prn
D:\GEOCIENCIAS V-12-2-DIC 2008\GEOCIENCIAS-VOL 12-2 DIC.vp
viernes, 20 de febrero de 2009 13:09:04

Composite 133 lpi at 45 degrees

Samples	Qtz	Pl	Kfs	Ms	Bt	Hbl	Cam	Grt	Ky	Sil	Tur	Ep	Accessories	Name; textures
01NC10	7	7	-	-	-	55	-	-	-	-	-	30	Czo, Rt, Spn	Amphibolite; Lepidoblastic
01NC15b	45	30	-	-	15	-	-	5	1	-	1	-	Zrn, Rt(3%), Ap, Chl	Grt-Ky schist; Lepidoblastic
01NC52a	40	35	-	-	20	-	-	2	-	1		-	Mnz, Ap, Rt, Ilm, Zrn, Gr	Grt-Sil gneiss; Lepidoblastic
01NC54	30	40	-	-	5	15	-	7	-	-	-	Tr	Zrn, Ilm(3%), Ap, Chl	Grt-Hbl schist; lepidoblastic
Melanosomes														
01NC2c	8	4		10	70	-	-	5	-	3	-	-		Bt schist; Lepidoblastic
01NC8b	7	Tr		Tr	3	-	90	-	-	-	-	-	Zrn, Ap, Rt, Ep	Amphibolite; Lepidoblastic
01NC40	3	Tr		2	95								Zrn, Ap	Bt schist; Lepidoblastic

WF = weak foliation
SF = strong foliation
IZ = Pl idioblastic zoning
MI = mirmekitic intergrowth
PI = perthitic intergrowth
FG = fine grained
MG = medium grained
CG = coarse grained
Peg. = pegmatitic
C = Concordant
D = Discordant

Mineral abreviation after Kretz (1983). All numbers are modes obtained mostly by visual comparison with mode estimation charts.

FEBRERO 20-GEOCIENCIAS-VOL 12-2 ULTIMA VERSION.prn
D:\GEOCIENCIAS V-12-2-DIC 2008\GEOCIENCIAS-VOL 12-2 DIC.vp
viernes, 20 de febrero de 2009 13:09:04

Composite 133 lpi at 45 degrees

Table 2. Whole rock analyses of Nason Ridge Migmatitic Gneiss lithologies, Cascades Core, WA.

	SiO_2	TiO_2	Al_2O_3	FeO	Fe_2O_3	MnO	MgO	CaO	Na_2O	K_2O	P_2O_5	LOI	Total
Leucosome													
01NC2a	70.3	0.19	16.1	n.d.	1.5	0.02	0.4	1.6	3.7	2.9	0.06	1.25	98.2
1NC2b	75.8	0.04	14.8	n.d.	0.9	0.00	0.2	1.2	4.3	1.6	0.03	1.23	100.1
01NC2c	78.8	0.05	12.3	n.d.	0.8	0.00	0.2	2.6	3.9	0.2	0.11	0.56	99.5
01NC3b	75.3	0.05	17.2	n.d.	0.8	0.00	0.2	1.5	3.4	2.4	0.04	1.17	102.0
01NC8a	71.28	0.285	16.21	1.84	0	0.03	0.94	2.55	3.96	2.05	0.1	0.97	100.2
01NC8c	74.24	0.064	15.16	0.86	0	0.008	0.23	3.05	5.28	0.72	0.02	0.78	100.4
01NC9a DK	69.9	0.38	17.1	n.d.	2.4	0.00	0.6	2.4	4.2	2.8	0.13	0.68	100.7
01NC9a LT	68.9	0.20	16.4	n.d.	1.6	0.00	0.4	2.1	3.8	3.1	0.08	0.86	97.4
01NC9b	72.7	0.08	16.0	n.d.	0.9	0.00	0.2	1.3	3.3	4.3	0.07	0.82	99.7
01NC40	72.1	0.14	16.6	n.d.	0.9	0.02	0.4	2.5	5.3	1.0	0.04	0.61	99.7
03NCHS3b	70.0	0.26	16.6	n.d.	2.4	0.00	1.0	2.6	4.3	0.8	0.06	0.37	98.4
Leucosome-lenses													
01NC15b	85.8	0.10	7.3	n.d.	1.9	0.00	0.3	1.5	1.7	0.3	0.07	0.39	99.3
01NC52a	81.1	0.07	10.1	n.d.	1.5	0.01	0.3	2.6	2.6	0.2	0.24	0.30	99.0
02NC7	79.8	0.03	11.8	n.d.	0.9	0.00	0.1	2.3	3.2	0.1	0.04	0.16	98.5
02NCout19	72.4	0.11	14.8	n.d.	2.1	0.01	0.5	3.2	4.5	0.5	0.07	0.44	98.6
03(99)NC57p	73.2	0.05	14.8	n.d.	1.2	0.00	0.4	4.4	4.5	0.3	0.72	0.23	99.9
03NCHS3b	76.0	0.06	15.2	n.d.	1.1	0.00	0.3	2.8	4.0	0.2	0.11	0.20	100.0

FEBRERO 20-GEOCIENCIAS-VOL 12-2 ULTIMA VERSION.prn
D:\GEOCIENCIAS V-12-2-DIC 2008\GEOCIENCIAS-VOL 12-2 DIC.vp
viernes, 20 de febrero de 2009 13:09:04

Composite 133 lpi at 45 degrees

	SiO_2	TiO_2	Al_2O_3	FeO	Fe_2O_3	MnO	MgO	CaO	Na_2O	K_2O	P_2O_5	LOI	Total
Mesosome													
96NC67(03)	62.5	0.81	17.3	n.d.	8.4	0.15	3.0	1.7	1.9	2.0	0.09	2.07	99.9
99NC37	66.5	0.78	15.8	5.32	0.7	0.11	2.9	1.7	2.0	2.3	0.17	1.10	99.4
01NC2-c	59.6	0.81	17.7	n.d.	7.7	0.13	2.8	2.4	3.4	3.0	0.26	2.05	99.8
01NC3-a	63.1	0.82	16.1	n.d.	7.4	0.10	3.0	2.2	3.2	2.9	0.17	0.98	100.1
01NC6	58.4	0.88	18.8	n.d.	8.1	0.11	3.1	2.6	3.3	2.6	0.20	2.76	100.9
01NC8d	48.3	2.28	13.3	10.09	2.6	0.23	6.33	12.0	1.4	0.7	0.22	0.87	98.3
01NC9c	65.6	0.72	15.8	n.d.	6.6	0.10	2.8	2.2	3.0	2.6	0.15	0.84	100.4
01NC9d	64.9	0.83	15.7	5.58	0.8	0.12	3.1	2.0	2.5	2.6	0.16	1.88	100.2
01NC15b	67.3	0.73	13.2	n.d.	6.5	0.08	2.6	2.4	2.4	1.7	0.17	1.39	98.4
01NC52a	60.3	0.89	18.3	n.d.	8.0	0.10	3.1	2.8	2.8	1.8	0.22	2.43	100.7
01NC54	49.6	1.64	21.2	9.7	1.9	0.25	2.5	7.6	3.4	0.9	0.16	0.27	99.2
02NC3b	64.1	0.78	16.0	n.d.	7.3	0.10	2.7	2.4	3.0	2.1	0.13	1.32	99.9
Melanosome													
01NC2c	45.8	1.8	22.6 4	n.d.	16.1	0.3	5.6	1.0	1.12	6.31	0.3	n.d.	101.1(dry)
01NC8b	54.4	0.21	8.4	6.41	1.1	0.24	13.9	10.6	0.8	0.7	0.17	1.58	98.6
01NC40	41.5	2.67	18.1	n.d.	17.7	0.14	7.8	0.5	0.4	8.4	0.33	2.20	99.8

(1) When no FeO is reported all iron is assumed as Fe^{3+}

All values reported as weight percent. Bulk-rock compositions were determined by X-ray fluorescence analysis of fused glass discs with The University of Alabama Phillips PW2400 X-ray fluorescence spectrometer equipped with a Rh X-ray tube. Calibration was based on 15 to 20 certified rock standards per element.

FEBRERO 20-GEOCIENCIAS-VOL 12-2 ULTIMA VERSION.prn
D:\GEOCIENCIAS V-12-2-DIC 2008\GEOCIENCIAS-VOL 12-2 DIC.vp
viernes, 20 de febrero de 2009 13:09:05

Composite 133 lpi at 45 degrees

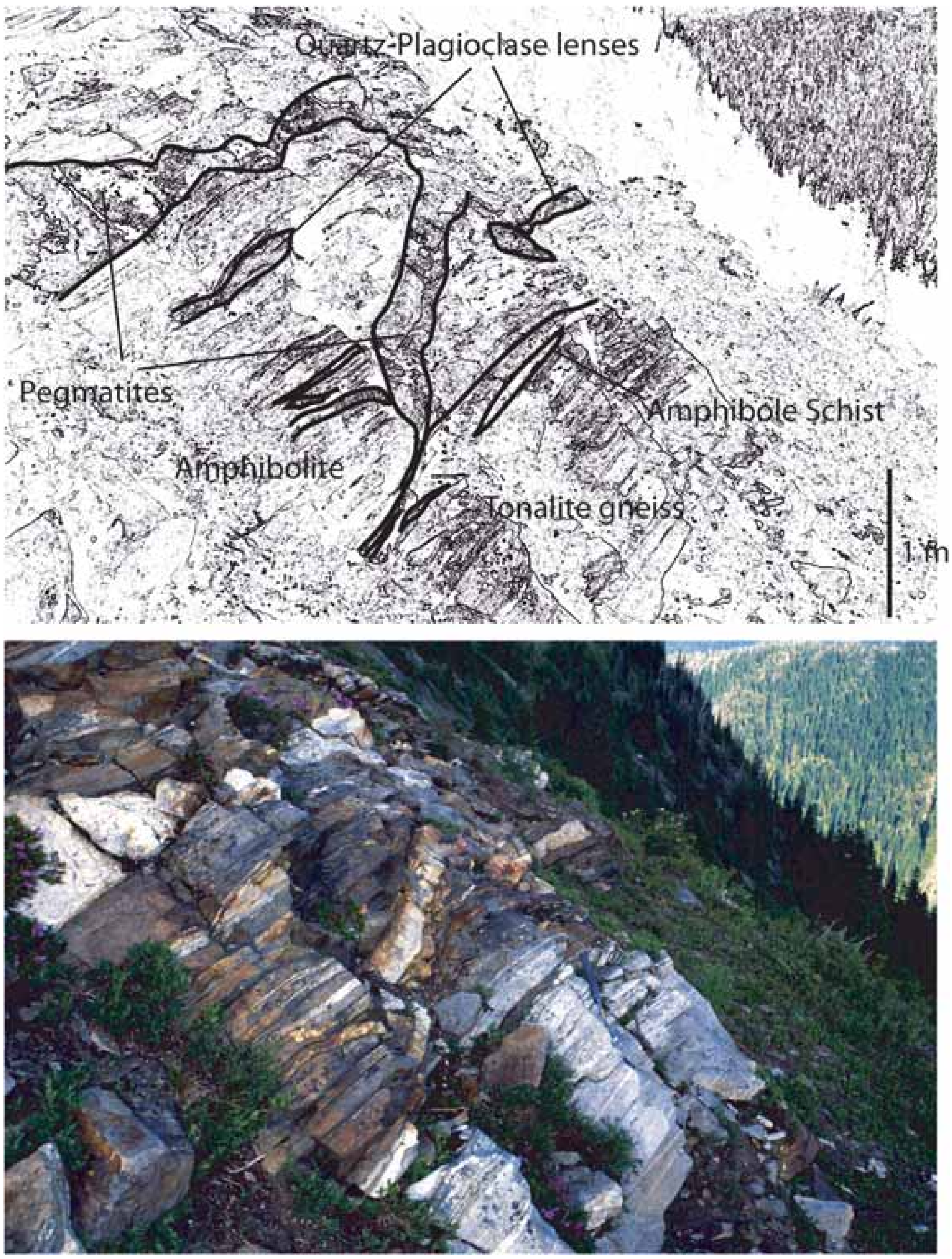

Figure 4. Outcrop photograph and sketch showing general relations between lithologies in the Nason Ridge Migmatitic Gneiss, Wenatchee Ridge, WA. Locality 01NC9 (see Fig. 2). The sledgehammer in the center of the picture is 0.4 m long. A thick amphibolite layer (~25 m) is observed above and left of a tonalite gneiss, these lithologies are cross-cut by pegmatites. Within the tonalite gneiss and just below teh amphibolite contact is observed a dark lens of amphibole schist.

FEBRERO 20-GEOCIENCIAS-VOL 12-2 ULTIMA VERSION.prn
D:\GEOCIENCIAS V-12-2-DIC 2008\GEOCIENCIAS-VOL 12-2 DIC.vp
viernes, 20 de febrero de 2009 13:09:06

Composite 133 lpi at 45 degrees

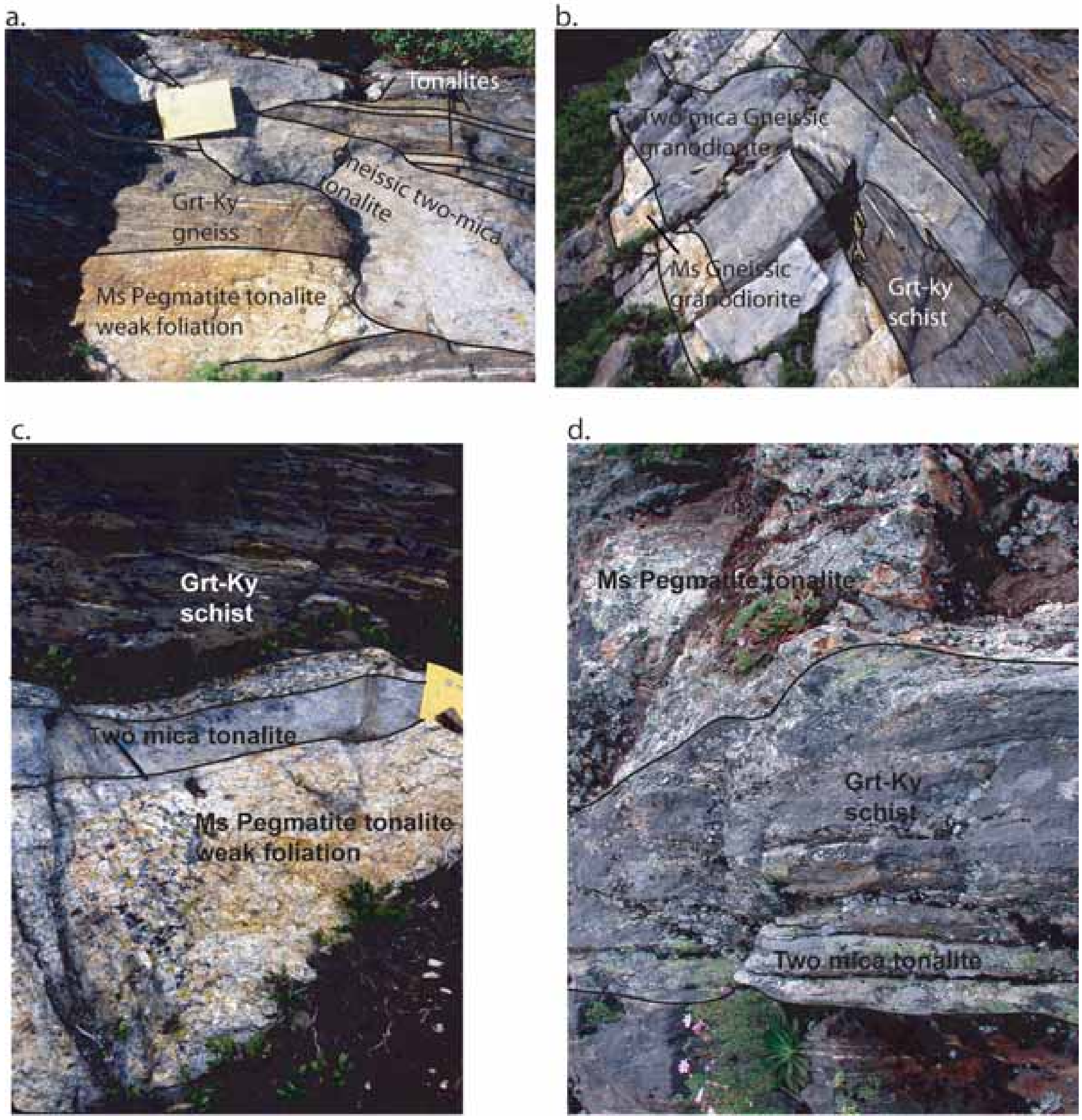

Figure 5. Examples of cross cutting relations between lithologies in the Nason Ridge Migmatitic Gneiss, Wenatchee Ridge, WA. a. A strongly-foliated tonalite crosscuting gneissose mesosome and weakly foliated tonalite. Note the two thin concordant non-foliated tonalites. b. Two foliated leucosomes interfingering with schistose mesosome. c. Weakly- to non-foliated leucosomes crosscutting schistose mesosome. d. Weakly-foliated pegmatite leucosome cross cutting schistose mesosome and weakly-foliated fine-grained tonalite concordant with schistose mesosome.

Leucosomes

Leucosomes include a variety of igneous-like lithologies, which have variable composition, textures, and field relations with other units (Figure 3; Tables 1 and 2). These units are generally tabular to sub-tabular in geometry and have thicknesses that range from cm to m scale (Figure 3). Three compositional groups are observed: 1) tonalites, 2) granodiorites, and 3) quartz-rich granitoids. Variation in the type of mica present (muscovite, biotite, or

FEBRERO 20-GEOCIENCIAS-VOL 12-2 ULTIMA VERSION.prn
D:\GEOCIENCIAS V-12-2-DIC 2008\GEOCIENCIAS-VOL 12-2 DIC.vp
viernes, 20 de febrero de 2009 13:09:08

Composite 133 lpi at 45 degrees

Table 3. Mineral chemistry, Nason Ridge Migmatitic Gneiss, Cascades Core (WA)

	01NC15b (Grt-Ky schist) Garnet Core - 5 anal.				**01NC52a (Grt-Sil Gneiss) Garnet core - 29 anal.**			
	Rep.	**Average**		**Cations**	**Rep.**	**Average**		**Cations**
	Oxides	**Oxides**	**s.d.**		**Oxides**	**Oxides**	**s.d.**	
SiO_2	36.72	36.71	0.09	2.96	37.01	37.13	0.16	2.96
TiO_2	0.11	0.22	0.23	0.01	0.02	0.05	0.10	0.00
Al_2O_3	21.32	21.20	0.20	2.02	21.63	21.74	0.15	2.05
Cr_2O_3								
FeO	26.13	26.45	0.29	1.78	28.81	28.71	0.20	1.93
MgO	1.33	1.33	0.02	0.16	2.18	2.30	0.06	0.28
MnO	5.81	5.59	0.16	0.38	5.32	5.30	0.12	0.35
CaO	8.05	8.06	0.24	0.70	5.18	5.33	0.13	0.45
Na_2O								
K_2O								
Total	99.47	99.56			100.15	100.56		
	02NC3b (Grt-Ky schist) Garnet core-20 anal.				**01NC8b (Amp. schist) Amphibole - 20 anal.**			
	Rep.	**Average**		**Cations**	**Rep.**	**Average**		**Cations**
	Oxides	**Oxides**	**s.d.**		**Oxides**	**Oxides**	**s.d.**	
SiO_2	36.78	36.55	0.15	2.95	47.81	47.90	0.43	6.93
TiO_2	0.15	0.14	0.02	0.01	0.28	0.30	0.03	0.03
Al_2O_3	21.13	21.31	0.13	2.03	11.23	10.94	0.38	1.86
Cr_2O_3					0.22	0.16	0.04	
FeO	27.38	27.44	0.23	1.85	8.55	8.43	0.22	1.02
MgO	1.21	1.25	0.04	0.15	14.68	14.70	0.20	3.17
MnO	5.16	5.16	0.08	0.35	0.28	0.27	0.03	0.03
CaO	7.98	7.91	0.15	0.68	11.81	11.91	0.15	1.85
Na_2O					1.02	1.04	0.07	0.29
K_2O					0.75	0.69	0.10	0.13
Total	99.80	99.76			96.63	96.33		

(1) The average of all analyses is reported together with the standard deviation and a representative analysis
(2) Oxides = oxide weight percent
(3) Cation are calculated based on 11 oxygens for biotite, 12 oxygens for garnet, 8 oxygens for plagioclase, and 23 oxygens for amphibole

FEBRERO 20-GEOCIENCIAS-VOL 12-2 ULTIMA VERSION.prn
D:\GEOCIENCIAS V-12-2-DIC 2008\GEOCIENCIAS-VOL 12-2 DIC.vp
viernes, 20 de febrero de 2009 13:09:09

Composite 133 lpi at 45 degrees

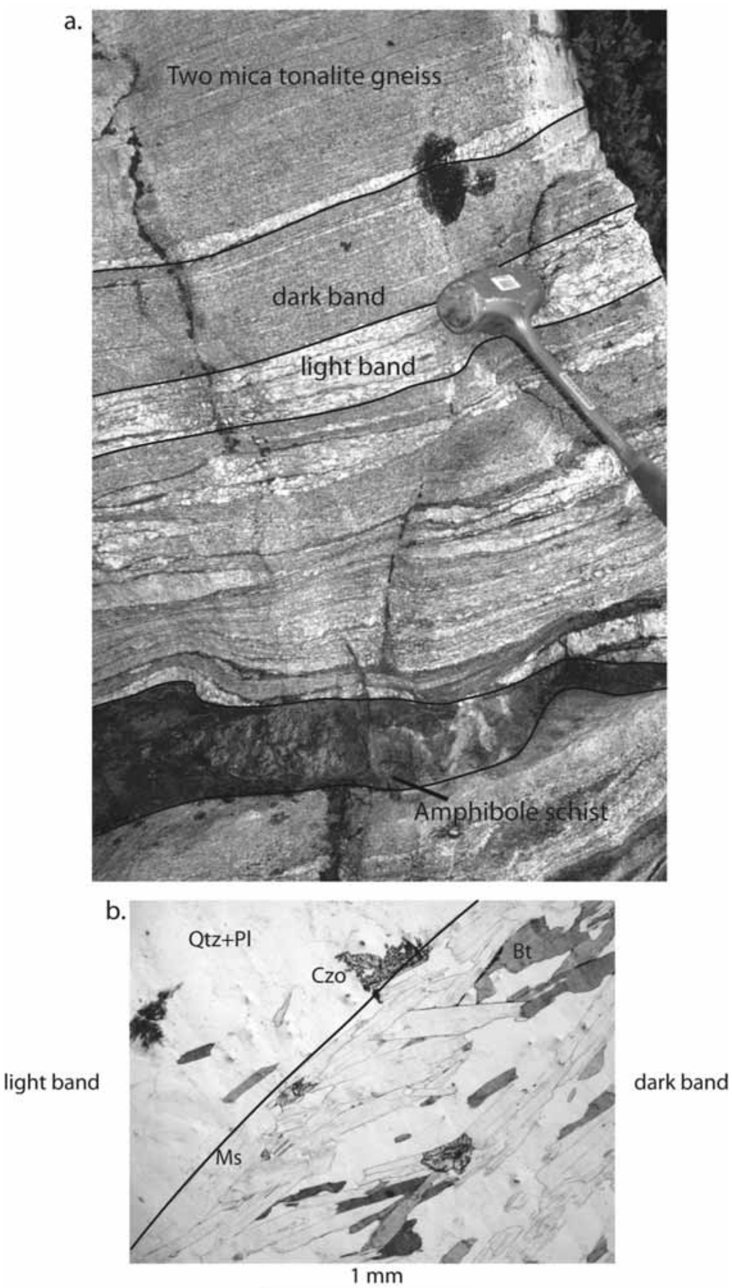

Figure 6. Characteristics of strongly foliated leucosomes, Nason Ridge Migmatitic Gneiss. Locality 01NC8. a. Compositional layering at cm scale observed in outcrop. b. Thin section photomicrograph of sample 01NC8a showing foliation defined by muscovite and biotite alignment, and compositional layering expressed as variable biotite content.

both) and variation in the content of mica, garnet, and tourmaline are the most definitive expression of compositional differences between groups. Texturally, these rocks can be differentiated on the basis of grain size and metamorphic foliation. Grain size is variable from fine grained to pegmatitic; pegmatites are tonalites to quartz-rich granitoids, but fine- to medium-grained leucosomes have a larger compositional range from granodiorite to tonalite. The degree of foliation development varies from almost non-foliated to gneissic. Foliation is defined by alignment of micas, compositional layering, and elongation of quartz and plagioclase. Compositional layering is more common within the thickest concordant gneissic leucosomes, where it is defined by variations in biotite content. Foliation in leucosomes is dominantly parallel to the regional trend of foliation observed in mesosomes (Figure 3).

Pegmatite leucosomes are non-foliated to weakly-foliated and generally crosscut mesosomes, but fine- to medium-grained leucosomes show both concordant and discordant relations with mesosomes (Figure 4 and Figure 5). Fine-grained leucosome bodies are weakly- to strongly foliated and show complex outcrop interrelationships, some weakly-foliated bodies crosscut strongly-foliated bodies (Figure 4) and some gneissic bodies crosscut weakly-foliated bodies (Figure 5a). Contacts with adjacent rocks are generally sharp and there is no evidence for contact metamorphism.

Small-scale relict igneous textures are common in pegmatite leucosomes, but are less common in

FEBRERO 20-GEOCIENCIAS-VOL 12-2 ULTIMA VERSION.prn
D:\GEOCIENCIAS V-12-2-DIC 2008\GEOCIENCIAS-VOL 12-2 DIC.vp
viernes, 20 de febrero de 2009 13:09:09

Composite 133 lpi at 45 degrees

finer grained rocks. These textures include idioblastic compositional zoning in plagioclase (most commonly simple zoning, and rarely oscillatory) and myrmekitic intergrowths of quartz and plagioclase.

Leucosome rock types are grouped, according to the degree of foliation development, into strongly foliated and weakly to non-foliated. This scheme emphasizes the variable deformation style and is readily applicable as objective criteria for field classification. Quartz-plagioclase lenses are grouped with weakly to non-foliated rocks because they do not show internal foliation features. Leucosome bodies with the exception of quartz – plagioclase lenses, constitute 16% to 43% of the outcrop area, along Wenatchee Ridge (Figure 2). The proprotion of these leucosomes drops to ca. 8% near the contact with the adjacent Chiwaukum Schist in the north.

Strongly-foliated rocks. Strongly-foliated leucosomes are both concordant (Figure 4) and discordant (Figure 5a) with mesosome fabrics. Mica alignment and alternating ferromagnesian-rich and quartz feldspathic-rich layers (Figure 6a) define foliation. Variation in biotite content at cm scale is the most notable expression of compositional layering (Figure 6b). Variation in grain size between layers is from fine- to medium-grained. This group of rocks ranges in composition from tonalite to granodiorite, contains one (muscovite) or two (muscovite + biotite) micas, and commonly contains: quartz + plagioclase + muscovite ± biotite ± garnet. Bulk rock chemical analyses (Table 2) reveals that these rocks are composed mainly of silica and aluminum (SiO_2+Al_2O_3 ~ 90%) and that they have low iron and magnesium contents (Fe_2O_3+MgO < 2%).

In general, these rocks are gneissic with granoblastic texture. Within the light colored biotite-poor layers, quartz-feldspar microlithons (< 0.2 cm) alternate with thin discontinuous muscovite microlithons (< 0.02 cm). Quartz is xenoblastic with arrested grain boundaries, undulatory extinction, and needle-like rutile inclusions aligned parallel to gneissosity. Plagioclase is xenoblastic or less commonly subidioblastic, regularly has idioblastic

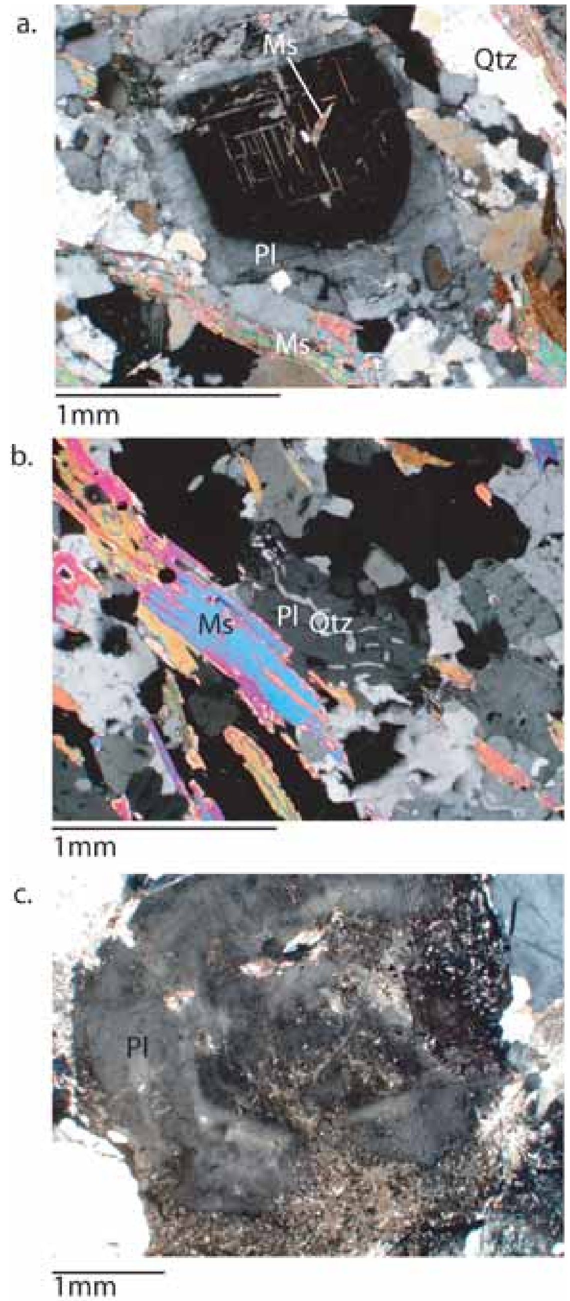

Figure 7. Photomicrographs illustrating relict igneous textures in leucosomes lithologies, Nason Ridge Migmatitic Gneiss, WA. a. Subidioblastic simple zoning in plagioclase. b. Quartz- plagioclase mirmekitic intergrowth. c. Idioblastic oscillatory zoning in plagioclase.

compositional zoning (Figure 7), and albite twinning. Pericline and Carlsbad twinning are rare. Plagioclase commonly contains relatively large muscovite grains

FEBRERO 20-GEOCIENCIAS-VOL 12-2 ULTIMA VERSION.prn
D:\GEOCIENCIAS V-12-2-DIC 2008\GEOCIENCIAS-VOL 12-2 DIC.vp
viernes, 20 de febrero de 2009 13:09:10

Composite 133 lpi at 45 degrees

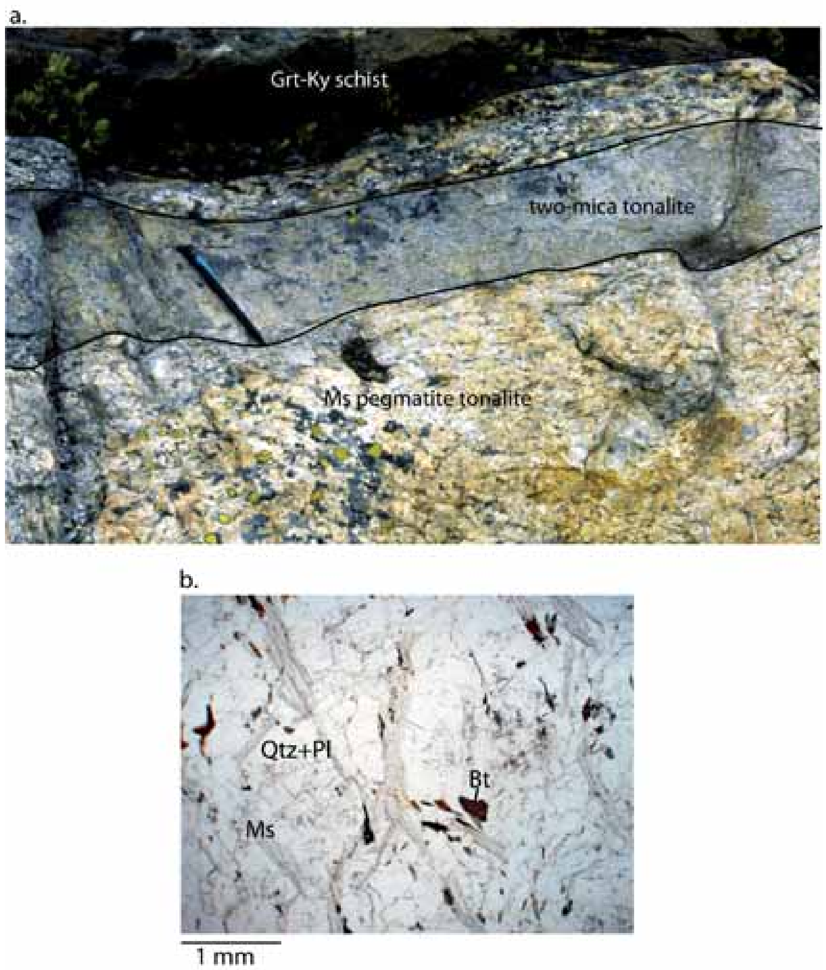

Figure 8. Characteristics of weak to non-foliated leucosomes, Nason Ridge Migmatitic Gneiss, WA. a. Outcrop aspect of a non-foliated (two-mica tonalite) and a weak foliated leucosome (muscovite pegmatite tonalite). b. Photomicrographs of the two-mica tonalite, no foliation is observed and mica grains are randomly orientated.

parallel to cleavage (Figure 7a), epidote, and occasionally quartz inclusions. Plagioclase can rarely be seen in vermicular intergrowths with quartz (Figure 7b). Potassium feldspar is xenoblastic and is pervasively altered to white mica (kaolinite, muscovite, and/or paragonite). Muscovite and biotite are subidioblastic and platy; both define gneissosity. Zircon inclusions are common in biotite. Garnet is an accessory phase, idioblastic to subidioblastic and nearly inclusions-free.

Weakly- to non- foliated rocks. These leucosome rocks are discordant and concordant bodies with compositions that range from tonalite to quartz-rich granitoid. Grain size varies from fine grained to pegmatitic (Figure 8a) and mineralogy is quartz + plagioclase + muscovite with biotite and garnet as minor to accessory phases. Quartz-plagioclase discontinuous lenses that occur in varying proportions within the gneisses and schists are grouped in this category. Chemically, these lithologies are very similar to strongly foliated bodies (Table 2), except the quartz – plagioclase lenses, which have lower Al_2O_3 content (~ 12%), slightly higher SiO_2 content, and slightly lower Fe_2O_3+MgO.

Weakly gneissose bodies have a granoblastic texture (Figure 8b). Quartz is xenoblastic with un-

FEBRERO 20-GEOCIENCIAS-VOL 12-2 ULTIMA VERSION.prn
D:\GEOCIENCIAS V-12-2-DIC 2008\GEOCIENCIAS-VOL 12-2 DIC.vp
viernes, 20 de febrero de 2009 13:09:12

Composite 133 lpi at 45 degrees

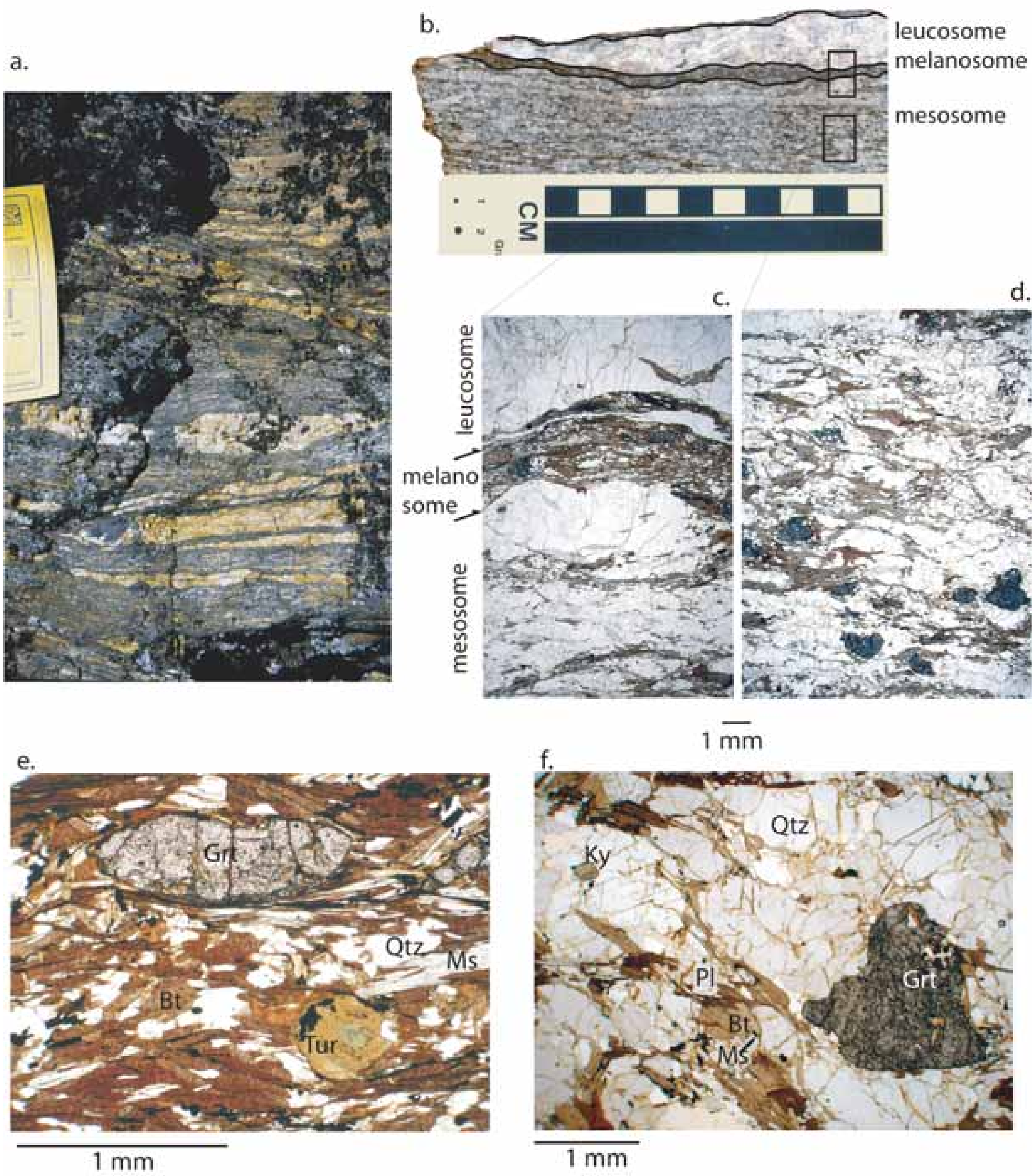

Figure 9. Characteristics of mesosome garnet-kyanite gneiss, sample 01NC2c, Nason Ridge Migmatitic Gneiss, WA. a. Layering at cm scale with abundant leucosome lenses. b. Thin melanosome layers are observed on each side of the leucosome lenses. c. Photomicrograph of the gneiss, mm scale leucosome, melanosome, and mesosome layers can be recognized. d. Photomicrograph under plane polarized light of the mesosome portion of the gneiss, observe the abundance of garnet. e. Photomicrograph of the melanosome portion, biotite, garnet, and quartz are the main components, tourmaline and muscovite are also present. f. Photomicrograph of the mesosome portion showing the most common mineral paragenesis: garnet + kyanite + quartz + plagioclase + biotite + muscovite.

FEBRERO 20-GEOCIENCIAS-VOL 12-2 ULTIMA VERSION.prn
D:\GEOCIENCIAS V-12-2-DIC 2008\GEOCIENCIAS-VOL 12-2 DIC.vp
viernes, 20 de febrero de 2009 13:09:13

Composite 133 lpi at 45 degrees

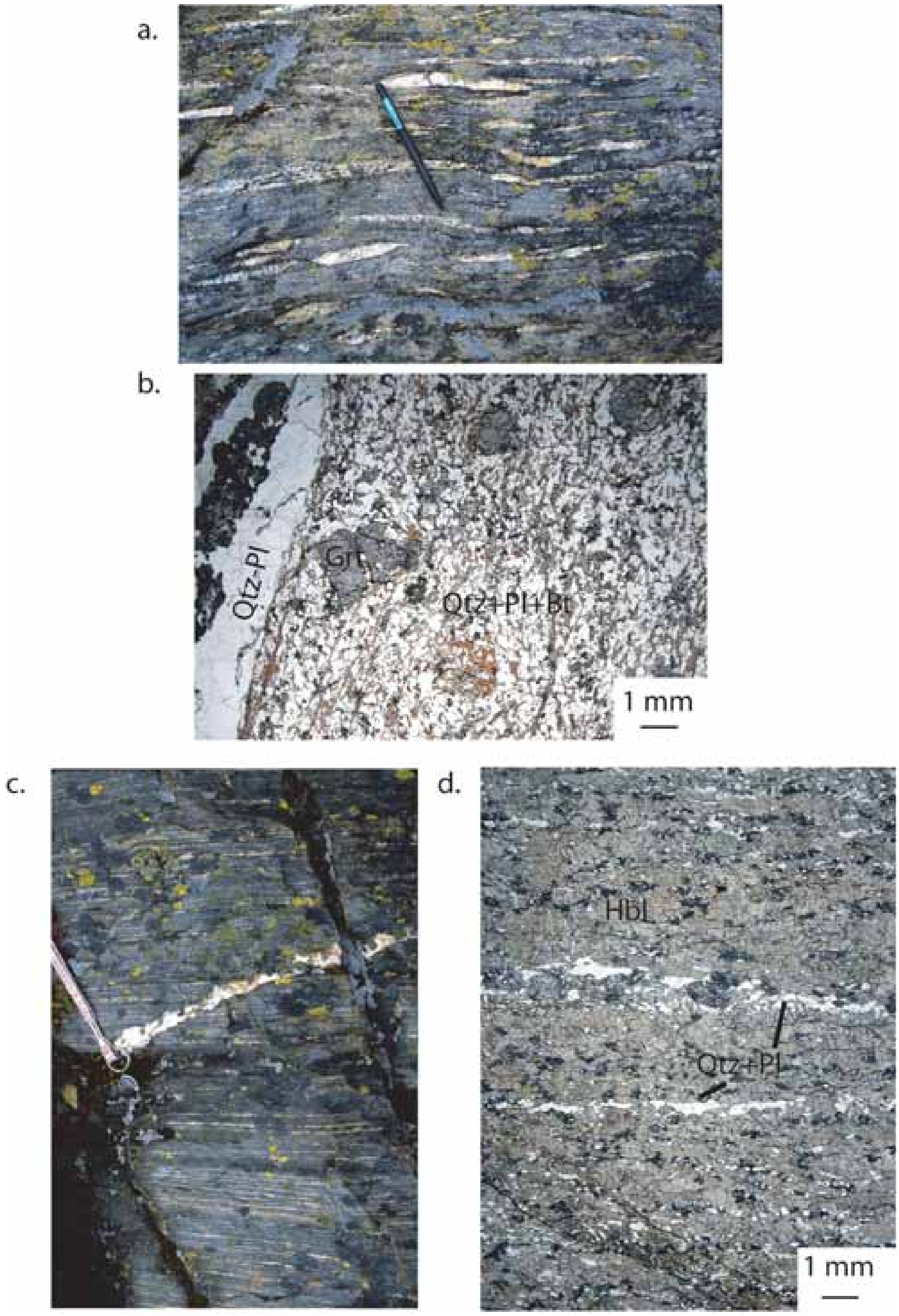

Figure 10. Characteristics of mesosome schist and amphibolite, Nason Ridge Migmatitic Gneiss, WA. a. Fine- to medium-grained with < 10% leucosome lenses. b. Photomicrograph in plane polarized light of a garnet-kyanite schist, note the large garnet porphyroblasts and the quartz-plagioclase lens (no associated selvage) in the lower portion of the photograph. c. Amphibolite layer with alternating dark hornblende-rich bands and thin light colored bands with quartz, plagioclase, and epidote. d. Photomicrograph of a garnet amphibolite composed mainly of hornblende, quartz, epidote, and small garnet porphyroblasts, sphene is accessory and observed evenly distributed.

FEBRERO 20-GEOCIENCIAS-VOL 12-2 ULTIMA VERSION.prn
D:\GEOCIENCIAS V-12-2-DIC 2008\GEOCIENCIAS-VOL 12-2 DIC.vp
viernes, 20 de febrero de 2009 13:09:15

Composite 133 lpi at 45 degrees

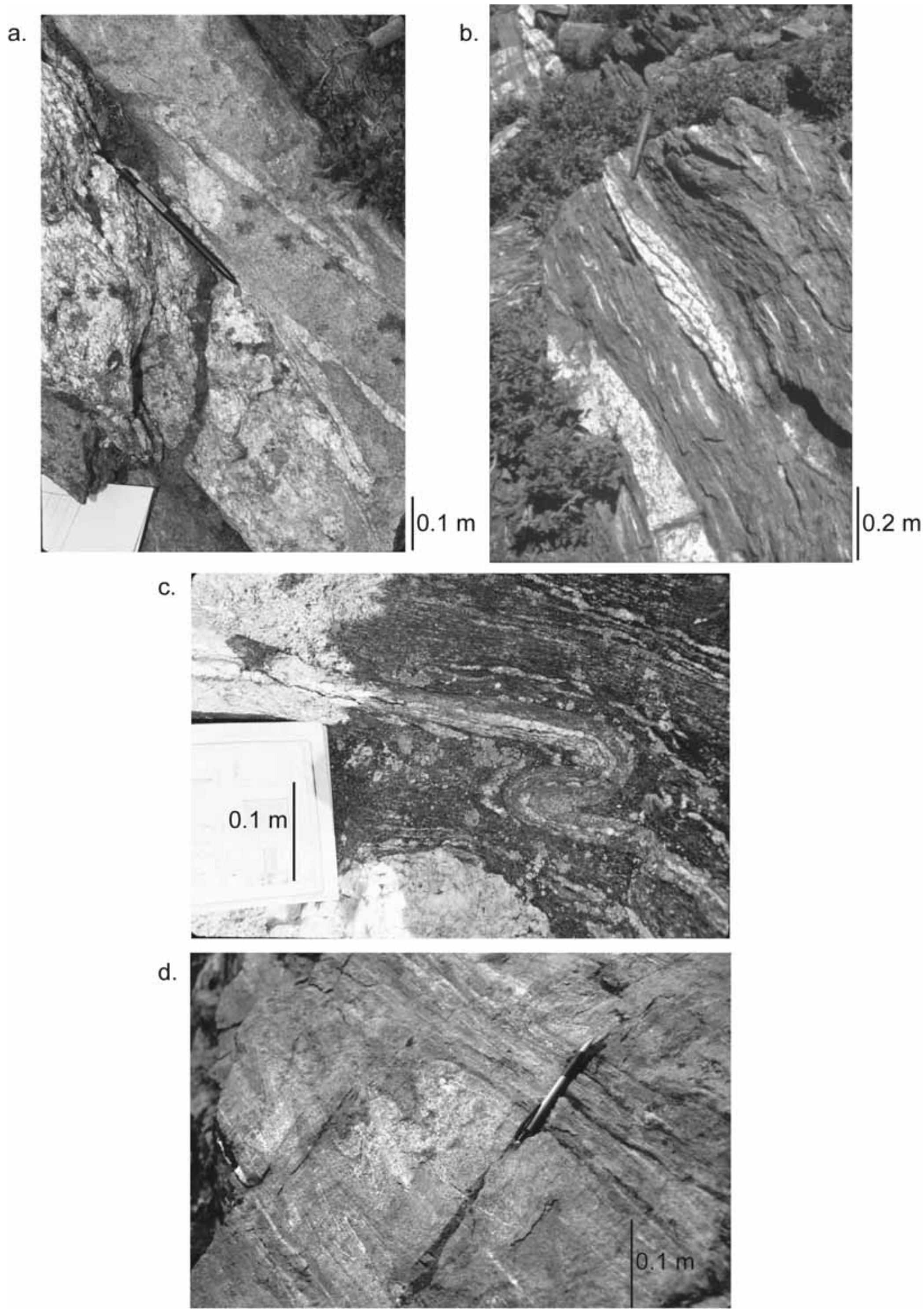

Figure 11. Mesoscopic structures observed on Wenatchee Ridge, WA. a. Quartz veins with tight isoclinal folding. b. Boudinage in pegmatite. c. Similar isoclinal folding in biotite-garnet-kyanite gneiss. d. Similar folding in biotite-garnet schist.

FEBRERO 20-GEOCIENCIAS-VOL 12-2 ULTIMA VERSION.prn
D:\GEOCIENCIAS V-12-2-DIC 2008\GEOCIENCIAS-VOL 12-2 DIC.vp
viernes, 20 de febrero de 2009 13:09:16

Composite 133 lpi at 45 degrees

dulatory extinction. Plagioclase is xenoblastic, but some small grains are subidioblastic with lath shape. Twinning is uncommon, but when present is pericline or rarely albite twinning. Quartz inclusions are common in plagioclase, and as in gneissic bodies, plagioclase is altered to muscovite along cleavage planes and in some cases to sericite, epidote, and clinozoisite. Muscovite is idioblastic to subidio- blastic, with platy form, and its alignment defines the gneissosity. Large grains of plagioclase and quartz have cracks filled with finer grained aggregates of quartz, muscovite, and plagioclase.

The quartz – plagioclase lens-shaped bodies have long dimensions of 0.05 to >1 m and are typically parallel or at low angle to the dominant foliation. They are composed mainly of quartz and plagioclase with minor amounts of biotite (Figures 9b and 9c). Quartz is xenoblastic and plagioclase is xenoblastic to subidioblastic. The plagioclase is commonly altered to muscovite and epidote. Quartz-plagioclase lenses are locally associated with thin discontinuous selvages of biotite-rich schist that are described below as melanosomes.

Melanosomes

Biotite schist. These thin (generally ≤ 2 cm thick) biotite-rich layers only occur directly adjacent to quartz-plagioclase leucosome lenses in the gneisses (Figure 9b). The mineral assemblage for these lenses is biotite + garnet + quartz + plagioclase ± muscovite ± tourmaline (Figure 9e). They are schistose with a strong lepidoblastic texture as a result of the high biotite content. Biotite is subidioblastic and tourmaline is idioblastic, other minerals present are generally xenoblastic. Garnet, when present, is generally strongly elliptical and elongate in the foliation orientation. The chemical composition of these rocks is controlled by the high biotite mode. The most important constituents are $SiO_2 + Al_2O_3 + Fe_2O_3 + MgO + K_2O + TiO_2$ (Table 2). SiO_2 content is notably lower than other Nason Ridge Migmatitic Gneiss lithologies and they have a high TiO_2 content (~2.7%).

Amphibole schist. Amphibole schist is coarse- to medium-grained and composed mainly of a calcic amphibole (Table 3). Other minerals present are quartz and plagioclase, and locally muscovite. The texture is strongly schistose and lepidoblastic (linear fabric defined by amphibole orientation). The amphibole is idioblastic with lamellar and simple twinning. It has abundant inclusions of quartz-plagioclase- muscovite-biotite, and is locally poikiloblastic. Quartz is xenoblastic with undulatory extinction, and fills voids between amphibole grains. Plagioclase is subidioblastic to xenoblastic. Muscovite is present mainly as inclusions in amphibole. These melanosome have also lower SiO_2 content that mesosomes or leucosomes (Table 2). Their chemical composition is similar to that of Biotite schist except that CaO is a major component and K_2O is a minor component.

Mesosomes

Mesosomes comprise schist, gneiss, and amphibolite. Gneiss described here as mesosome is compositionally distinct from leucosome gneiss, has contacts that are concordant with adjacent mesosome schists, and differs from mesosome schist only by containing lesser amounts of biotite. Mesosome gneiss differs mineralogically from leucosome gneiss in that it contains abundant garnet and kyanite.

Schist and gneiss. Fine- to medium-grained schist and medium grained gneiss with porphyroblasts of kyanite (1 – 5 mm), garnet (1 – 30 mm), and tourmaline (< 2 mm). The most common prograde mineral assemblage is biotite + quartz + plagioclase with variable amounts of muscovite, garnet, staurolite, and kyanite/sillimanite. Accessory phases include tourmaline, apatite, rutile, ilmenite, and zircon. Chemical composition of schist and gneiss is characterized by SiO_2 between 60 and 70%, Al_2O_3 between 13 and 18%, Fe_2O_3 between 6 and 8%, and $MgO+CaO+Na_2O+K_2O$ between 2 and 4% (Table 2). Mesosome gneiss is chemically different from leucosome gneiss in that Fe_2O_3+MgO is greater than 9% and SiO_2 is lower than 70% in mesosomes while Fe_2O_3+MgO is lower than 3% and SiO_2 is greater than 70% in leucosomes. Gneiss shows compositional layering at mm scale with alternating biotite-rich and biotite-poor layers, and at cm scale

FEBRERO 20-GEOCIENCIAS-VOL 12-2 ULTIMA VERSION.prn
D:\GEOCIENCIAS V-12-2-DIC 2008\GEOCIENCIAS-VOL 12-2 DIC.vp
viernes, 20 de febrero de 2009 13:09:17

Composite 133 lpi at 45 degrees

with < 2 cm thick leucosome lenses bounded by < 0.5 cm thick melanosome layers (Figure 9). Compositional layering is also expressed by subtle variations in garnet and kyanite content, and porphyroblast size. Schist contains quartz-plagioclase leucosome lenses of < 10% with lengths from 2 cm to 10 cm and thickness < 5 mm (Figure 10a).

Mineral alignment is commonly observed in hand sample and includes parallel orientation of mica (defining foliation) and sub-parallel orientation of kyanite and tourmaline porphyroblasts (defining lineation). Foliation along the crest of Wenatchee Ridge generally strikes west-northwest and dips north-northeast (Figure 2 and Figure 3). Lineation is subhorizontal west trending (Figure 3). Other fabrics observed at thin section and outcrop scale include asymmetric augen and microfolding to mesofolding with axial surfaces parallel to subparallel with foliation (Figure 11). At the microscopic scale penetrative foliation is characterized by parallel orientation of biotite and muscovite grains. Locally, garnet porphyroblasts have helicitic snowball structures compatible with rotation and large biotite grains have mica fish morphology also compatible with porphyroblast rotation. Gneiss has lepidoblastic texture in melanosomes, granoblastic texture in leucosomes, and granoblastic predominating over lepidoblastic textures in mesosomes (Figure 9). Schist varies from strongly schistose to weakly gneissose, with subtle compositional layering formed by quartz-rich lenses and varying amounts of biotite. Grain contacts show generally arrested morphology, but some minerals are subidioblastic to idioblastic with well-developed faces (especially porphyroblasts). Muscovite and chlorite occur as retrograde minerals that commonly crosscut foliation and/or form epitaxial intergrowths with biotite. Muscovite is also present in some layers apparently as a prograde mineral. Quartz is fine-grained to locally coarse, xenoblastic, and in some cases elongated in the foliation direction, with undulatory extinction and abundant fractures probably reflecting late brittle features. Plagioclase is fine-grained, xenoblastic to subidioblastic with irregular shape, but a few laths are observed. Pericline and albite twinning are common, and carlsbad twinning is rare. Simple idioblastic compositional zoning is observed in some grains, with an inclusion rich albitic core. Larger grains contain rounded inclusions of quartz. Locally, plagioclase is altered to muscovite and epidote. Biotite is subidioblastic, deep brown in color, contains abundant zircon inclusions, and a lesser number of apatite and opaque mineral grains. Biotite preferred orientation generally defines the dominant foliation. In some rocks, biotite is replaced by chlorite in epitaxial intergrowth. Muscovite is subidioblastic and most commonly occurs as fine aggregates of randomly oriented grains replacing kyanite porphy- roblasts. Garnet is xenoblastic to subidioblastic in gneisses (Figure 13, Figure 14, and Figure 15) and idioblastic to subidioblastic in schists. Locally garnet is poikiloblastic, and elongated parallel to the foliation. Poikiloblastic crystals contain inclusions of quartz, plagioclase, and biotite, and are surrounded by coronas or pressure shadows of quartz- plagioclase aggregates. X-ray maps and quantitative mineral analyses across grains indicate that xenoblastic to subidioblastic garnet grains generally have weak compositional zoning while other subidioblastic to idioblastic garnet grains have strong compositional zoning. Weakly-zoned garnet displays smooth zoning profiles with no significant central zoning and with relatively wide (> 0.2 mm) rims with increased spessartine mole fraction and Fe/(Fe + Mg) (Figure 12b) which is refer to as reverse zoning to indicate that this pattern is the reverse to that which would be predicted for growth during increasing temperatures (Hollister, 1966). The lack of strong central zoning and wide ‘reverse’ zoned rims in these subidioblastic to xenoblastic grains is interpreted to result from post-growth diffusion and partial resorption. Strongly zoned garnet grains have smooth bell-shaped zoning profiles and wide to thin reverse zoned rims. Almandine and pyrope mole fractions show enrichment from core to rim (X_{alm} ~0.60 to ~0.73, X_{prp} ~0.05 to ~0.18), and spessartine and grossular mole fractions are correspondingly depleted (X_{spss} ~0.15 to ~0.02, X_{grs} ~0.23 to ~0.09). A reversal in zoning is also present near the rims, but this is typically a zone less than 0.1 mm wide. The strong zoning in these subidioblastic to idioblastic grains is interpreted to re-

FEBRERO 20-GEOCIENCIAS-VOL 12-2 ULTIMA VERSION.prn
D:\GEOCIENCIAS V-12-2-DIC 2008\GEOCIENCIAS-VOL 12-2 DIC.vp
viernes, 20 de febrero de 2009 13:09:17

Composite 133 lpi at 45 degrees

sult from growth during prograde metamorphism. Grain size distribution for garnet is bimodal with a median for larger grains between 1-3 mm and a median for smaller grains at ~0.1 mm. Larger grains generally have abundant inclusions of quartz, plagioclase, biotite, muscovite, ilmenite, and graphite. Smaller garnet grains generally lack inclusions. Kyanite is idioblastic to subidioblastic, bladed with an orientation parallel to foliation, and varies from pristine in some samples to completely replaced by muscovite in others. Sillimanite is present as prismatic, isolated, less than 5 mm long grains and as aggregates of fibrolite. Chlorite only occurs as a retrograde mineral replacing biotite. Tourmaline is acicular idioblastic, aligned with foliation, and color zoned (green core – brown rim).

Amphibolite. Amphibolite varies from fine to medium grained layers that are up to 25 m thick (Figure 2 and Figure 4). The typical mineral assemblage is hornblende + quartz + plagioclase ± garnet ± sphene ± epidote ± zoisite (Fig. 10d). Bulk rock chemical analysis for one amphibolite sample reveals that their SiO_2 content is lower than 50% and that they have higher Fe_2O_3+MgO (> 25%) and CaO (> 12%) than other mesosome lithologies (Table 2). The texture is schistose with compositional layering characterized by alternating light green quartz-plagioclase-epidote and dark green hornblende-rich layers (Figure 10c and Figure 10d). Dark green layers have lepidoblastic texture defined by hornblende alignment. Quartz-rich lenses with granoblastic texture are commonly present. Hornblende is idioblastic to subidioblastic in elongated prisms defining schistosity. It contains abundant inclusions of quartz and epidote that are poorly aligned with schistosity. Epidote is equant xenoblastic to subidioblastic. Plagioclase is xenoblastic to subidioblastic (in quartz-rich lenses), strongly altered to muscovite-epidote-clinozoisite, but albite twinning and a subidioblastic zoning are still recognizable. Quartz is present as a minor phase mainly filling spaces between amphiboles. Sphene is diamond shaped, idioblastic, and regularly distributed. Garnet is equant, poikiloblastic and xenoblastic, concentrated in hornblende-rich layers, and has abundant inclusions of plagioclase, quartz, and epidote.

Interpretation of textural features

The Nason Ridge Migmatitic Gneiss leucosomes described above (non-foliated to weakly-foliated pegmatites and tonalites, strongly-foliated tonalites, and quartz-plagioclase lenses) are interpreted as: undeformed (some pegmatites), weakly deformed (some pegmatites and tonalites), and strongly deformed (tonalite gneiss). These differing amounts of deformation likely reflect emplacement of magmatic bodies over a protracted period of time during variable states of stress. Unfortunately, no geochronological data are available to quantify the timing and duration of emplacement. The non-foliated quartz-plagioclase lenses define foliation in mesosomes and thus were probably affected by or related to the deformation event that produced foliation in the strongly deformed tonalite gneiss. They are also locally rimmed with selvages composed mainly of biotite and garnet. These textural features support the local development of partial melts (quartz-plagioclase lenses) from mesosome lithologies. Segregation of melt into the lenses would leave behind an un-melted restite. There are no other unambiguous textures supporting partial melting; however, low generation of partial melts hindered melt segregation and extensive deformation and metamorphic re-equilibration subsequent to melting could have erased other partial melting textures.

Nason Ridge Migmatitic Gneiss rocks show variable evidence for retrogression. The most commonly observed retrograde features are poikiloblastic garnet with wide rims of reverse or retrograde zoning, kyanite partially or completely replaced by muscovite, and chlorite replacing Fe-Mg minerals. Wide (up to 0.2 mm) rims of manganese enrichment and increased Fe/(Fe+Mg) are interpreted to represent resorption of garnet. Manganese that was preferentially incorporated into garnet during growth is inferred to have been re-incorporated into remaining garnet near the rim during consumption of the grain. Other components in the garnet are distributed into matrix phases, and there likely was Fe-Mg exchange with other matrix minerals and equilibration associ-

FEBRERO 20-GEOCIENCIAS-VOL 12-2 ULTIMA VERSION.prn
D:\GEOCIENCIAS V-12-2-DIC 2008\GEOCIENCIAS-VOL 12-2 DIC.vp
viernes, 20 de febrero de 2009 13:09:17

Composite 133 lpi at 45 degrees

ated with diffusion of these elements into the garnet at high temperature.

Melanosome origins have been interpreted in several ways (Brown, 2002; Kriegsman, 2001). The most common interpretation for melanosomes is that they are sites of melt extraction, and represent the non-reactive un-melted fraction of the rock or restite (Mehnert, 1968; Brown *et al.*, 1995). A second interpretation, which has received recent attention, is that melanosomes result from retrograde back reactions between crystallizing melt (leucosome) and host rock (Kriegsman and Hensen, 1998; Kriegsman, 2001). A third interpretation is that melanosomes are formed by mafic minerals crystallizing from a melt (Kriegsman, 2001). The interpretation that selvages are an un-melted fraction is disregarded here based on thermodynamic modeling (see Chapter 3). Although, as predicted by modeling, the probable melting reactions involve very little biotite and the resulting melts would have low iron and magnesium, back-reactions during partial melt crystallization and retrograde metamorphism would produce biotite modal increase in restite rimming leucosomes. An argument against formation of selvages by back-reactions is that they are not always observed around leucosome lenses, even within the same mesosome lithologies. It seems reasonable, if retrogression was an extensive selvage forming mechanism, that the melanosome would be present around all leucosome lenses in the Nason Ridge Migmatitic Gneiss. However, the biotite selvage forming mechanism envisioned here requires that the volume of equilibration between leucosome and restite must be close to a 1:1 proportion or higher (see Figure 11, Chapter 3) and that this back-reactions focused on a thin layer surrounding the segregated melt. If back-reactions are taking place between equal proportions of leucosomes and restite in a larger scale (not focusing in mm to cm rimming restite) modal proportion of biotite will be uniform across the re-equilibrated portion of the rock and no biotite-rich rimming selvage will be observed.

Sharp contacts between leucosome gneiss and adjacent rocks and the strongly deformed character of the gneiss suggest that these bodies were emplaced as magmas before the last deformation event. These rocks most probably formed by injection of foreign magma because the volume of magma (up to 43%) is too great to have formed locally. There is a general absence of evidence for contact metamorphism around leucosomes; however this is readily explained by overprinting of later metamorphic events (M_3^R) and/or by small temperature differences between the igneous bodies and the country rock. The origin of discordant weakly foliated leucosome is uncertain, because they could have originated by partial melting at lower crustal levels within the same unit, then traveled short distances to their emplacement position.

P-T paths for metamorphism in the Nason Ridge Migmatitic Gneiss

Three *P-T* paths from NRMG (see Stowell et al., 2007) based on metamorphic peak *P-T* estimates from thermobarometry and pseudosections and initial garnet growth *P-T* estimations from garnet chemistry compositions plotted in *P-T* pseudosections show that garnet initial growth was in all samples in a range of 550 ºC ± 25 °C, and 6.5 kbar ± 1 kbar; estimated peak *P-T* conditions are, however, variable and they are evidence of the degree of exhumation of a particular area. The finite *P-T* paths reflect a pressure increase during garnet growth of less than 2 kbar (Figure 12) in agreement with other estimates in the NRMG and the nearby Chiwaukum Schist.

Pseudosection models of partial melts in metapelitic rocks of the Nason Ridge Migmatitic Gneiss

Pseudosection models of two samples from the NRMG (Zuluaga, 2004) support wet partial melting as the origin for leucosome lenses and associated biotite selvages. Water likely saturated the system during metamorphism and partial melting as indicated by *T-X*(H_2O) pseudosections. Temperature predictions for wet partial melting, using *P-T* pseudosections, are in the range of 655 ºC (10 kbar) – 703 ºC (3 kbar); melts were produce likely by reactions that involve comsumption of quartz and plagioclase. *P-T* pseudosection predictions also in-

FEBRERO 20-GEOCIENCIAS-VOL 12-2 ULTIMA VERSION.prn
D:\GEOCIENCIAS V-12-2-DIC 2008\GEOCIENCIAS-VOL 12-2 DIC.vp
viernes, 20 de febrero de 2009 13:09:17

Composite 133 lpi at 45 degrees

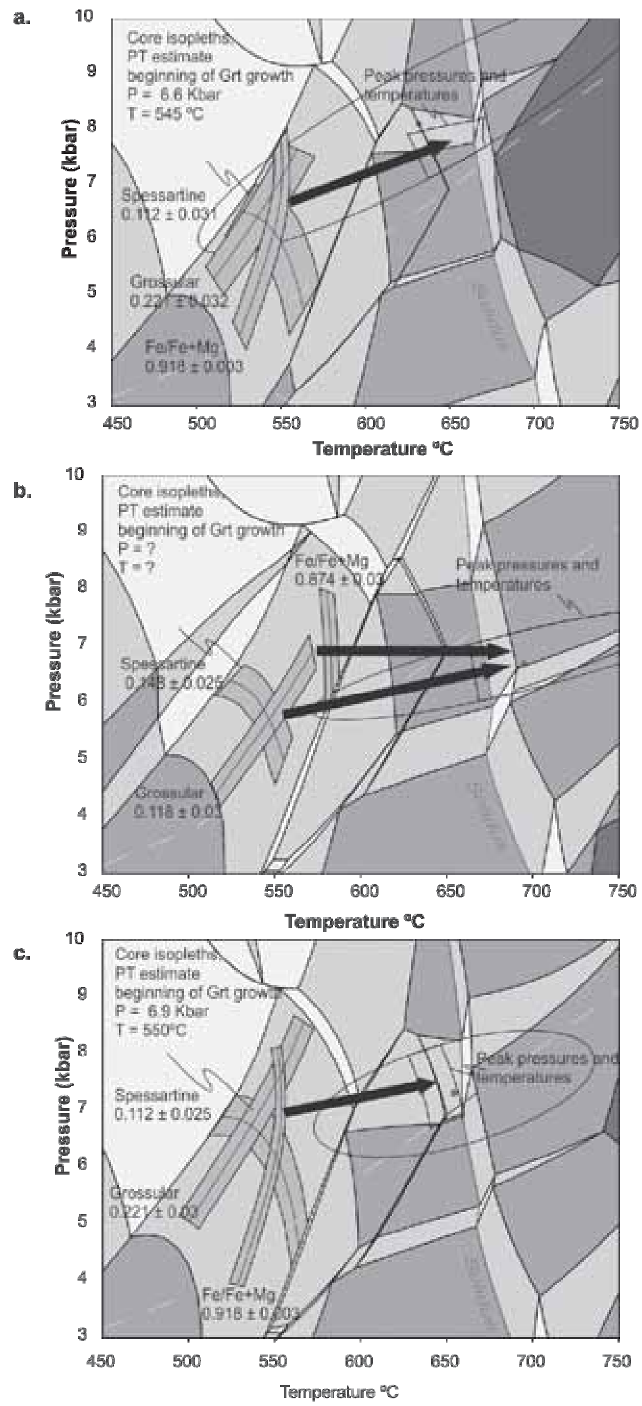

Figure 12. Metamorphic P-T paths for Nason Ridge Migmatitic Gneiss, WA. Garnet rim and core P-T estimates plotted on the MnNCKFMASH P-T pseudosection define the garnet growth segment of the path. Final 'peak' P-T for garnet growth is estimated from garnet near-rim compositions and matrix mineral chemistry using avergae P-T with THERMOCALC. The intersection of the uncertainty ellipse for rim thermobarometry with the fields for the peak mineral assemblage provides the best estimation of peak metamorphic conditions. a. Sample 01NC15b (Wenatchee ridge). b. Sample 01NC52a. (Pacific crest) c. Sample 02NC3b (Nason ridge).

FEBRERO 20-GEOCIENCIAS-VOL 12-2 ULTIMA VERSION.prn
D:\GEOCIENCIAS V-12-2-DIC 2008\GEOCIENCIAS-VOL 12-2 DIC.vp
viernes, 20 de febrero de 2009 13:09:19

Composite 133 lpi at 45 degrees

clude production of leucocratic melts, peritectic garnet, and peritectic kyanite, and consumption of biotite and muscovite. Predictions are also consistent with the presence of biotite selvages as product of retrograde back-reactions (Zuluaga, 2004; see also Kriegsman, 2001).

Discussion

Four general models have been proposed to explain the origin of migmatitic rocks: metamorphic differentiation, metasomatism, injection of foreign magma, and partial melting. Metasomatism was inferred for formation of the Nason Ridge Migmatitic Gneiss by Van Diver (1967). Later, other authors have inferred that this unit originated mainly from magmatic injection (Miller and Patterson, 2001). Results from thermodynamic modeling and petrographic observations suggest that partial melting was responsible for some of the leucosomes observed within the Nason Ridge Migmatitic Gneiss. Water content and temperature are the two most important variables controlling the formation of partial melts. In the model presented in chapter 3, water is assumed to be the product of dehydration reactions and that remained in the system (closed system) or it was sequentially expulsed from the system during prograde metamorphism (open system). Lack of water availability would cause low volumes of partial melt and unlikely preservation of partial melting textures because of metamorphic re-equilibration. Temperature estimates for Nason Ridge Migmatitic Gneiss (625 ºC – 806 ºC) are close to or above the estimated wet solidus (655 ºC at 10 kbar – 703 ºC at 3 kbar). Estimated peak metamorphic conditions and rock textures for sample 01NC52a support a partial melt origin for leucosome quartz – plagioclase lenses. In outcrops close to sample 01NC15b locality textures are also compatible with partial melt origin for quartz – plagioclase lenses. However, estimated peak metamorphic conditions for this sample are at temperatures lower than those predicted for initiation of melting. This discrepancy may be explained by back-reactions that are modeled thermodynamically in Chapter 3, where the absence of textures indicative of partial melting are explained by low melt generation at some levels that hindered melt segregation and allowed retrograde re-equilibration.

The *P-T* paths calculated for samples 01NC15b and 02NC3b are similar to *P-T* paths determined in the nearby Chiwaukum Schist (Tinkham, 2002), where *P-T* paths show zero to ≤ 2 kbar pressure increase during garnet growth. The *P-T* path for sample 01NC52a is not well constrained; however, the possible *P-T* paths in this sample are consistent with the interpretation of paths with less than 2 kbar pressure increase. Results show considerably smaller pressure increases than those proposed by previous workers (e.g., Brown and Walker, 1993; Whitney *et al.,* 1999).

The working hypothesis proposed for the Nason Ridge Migmatitic Gneiss origin include three events: pre- to syn-tectonic intrusives (gneissic tonalites), melting with formation of leucosome lenses, veins and patches, and a late intrusive event, that might or might not be related to partial melting of the same unit at lower crustal levels. The concordant character and the strong foliation interpreted to have resulted from the main deformation event are the arguments supporting a pre- to syn-tectonic intrusion origin for the gneissic tonalites. The presence of selvages and thermodynamic model predictions suggest partial melting for the origin of discontinuous leucosome lenses present in Nason Ridge Migmatitic Gneiss lithologies. These lenses did not form an interconnected net of melt and thus partial melts generated at this crustal level did not migrate far from the melting site. The interconnected array of pegmatites and weakly foliated tonalites are probably of post- or syn-tectonic origin.

Acknowledgements

Bob Miller and Scott Patterson are thanked for their generous help during field work. NSF EAR–9628232 (Green and others) and NSF EAR–0207777 (Stowell) provided partial analytical and field support. The University of Alabama Hooks fund, The University of Alabama Mobil fund, The University of Alabama graduate student association research fund, the Geological Society

FEBRERO 20-GEOCIENCIAS-VOL 12-2 ULTIMA VERSION.prn
D:\GEOCIENCIAS V-12-2-DIC 2008\GEOCIENCIAS-VOL 12-2 DIC.vp
viernes, 20 de febrero de 2009 13:09:19

Composite 133 lpi at 45 degrees

of America, and the southeastern section of the Geological Society of America provided direct support to Carlos Zuluaga for this research.

References

Armstrong, J.T. (1984) Quantitative analysis of silicate and oxide minerals: A reevaluation of ZAF corrections and proposal for new Bence-Albee coefficients. Microbeam Analysis, 208-212.

Ashworth, J.R. and McLellan, E.L. (1985) Textures: in Ashworth, J.R., editors, Migmatites. Blackie, Glasgow, 180-203.

Brown, E.H. and Talbot, J.L. (1989) Orogen-parallel extension in the North Cascades crystalline core, Washington. Tectonics, 8, 1105-1114.

Brown, E.H. and Walker, N.W. (1993) A magma loading model for Barrovian metamorphism in the Southeast Coast Plutonic Complex, British Columbia and Washington Geological Society of America Bulletin, 105, 479-500.

Brown, E.H., Cary, J.A., Dougan, B.E., Dragovich, J.D., Fluke, S.M., and McShane, D.P. (1994) Tectonic evolution of the Cascades Crystalline Core in the Cascade River area, Washington. Washington Division of Geology and Earth Resources Bulletin, 80, 93-113.

Brown, M. (2002) Retrograde processes in migmatites and granulites revisited. Journal of Metamorphic Geology, 20, 25-40.

Brown, M., Arvekin, Y.A., McLellan, E.L., and Sawyer, E.W. (1995) Melt segregation in migmatites. In Brown, M.; Rushmer, T.; Sawyer, E.W., editors, Mechanisms and Consequences of Melt Segregation from Crustal Protoliths. Journal of Geophysical Research, B 100, 15655- 15679.

Evans, B.W. and Berti, J.W. (1986) Revised metamorphic history for the Chiwaukum Schist, North Cascades, Washington, Geology, 14, 695-698.

Evans, B.W. and Davidson, G.F. (1999) Kinetic control of metamorphic imprint during synplutonic loading of batholiths; an example from Mount Stuart, Washington. Geology, 27, 415-418.

Haugerud, R.A., Van, d. H.P., Tabor, R.W., Stacey, J.S., and Zartman, R.E. (1991) Late Cretaceous and early Tertiary plutonism and deformation in the Skagit gneiss complex, North Cascade Range, Washington and British Columbia. Geological Society of America Bulletin, 103, 1297-1307.

Holland, T.J.B. and Powell, R. (1998) An internally consistent thermodynamic data set for phases of petrological interest. Journal of Metamorphic Geology, 16, 309-343.

Holland, T.J.B. and Powell, R. (2001) Calculation of phase relations involving haplogranitic melts using an internally consistent thermodynamic dataset. Journal of Petrology, 42, 673-683.

Hollister, L.S. (1966) Garnet zoning: an interpretation based on the Rayleigh fractionation model. Science, 154, 1647-1651.

Kretz, R. (1983) Symbols for rock-forming minerals. American Mineralogist, 68, 277-279.

Kriegsman, L.M. (2001) Partial melting, partial melt extraction, and partial back reaction in anatectic migmatites. Lithos, 56, 75-96.

Kriegsman, L.M. and Hensen, B.J. (1998) Back reaction between restite and melt: implications for geothermobarometry and pressure-temperature paths. Geology, 26, 1111-1114.

Magloughlin, J.F. (1986) Metamorphic petrology, structural history, geochronology, tectonics, and geothermometry/geobarometry in the Wenatchee Ridge area, North Cascades, Washington. University of Washington, Master Science thesis, 344 p.

Magloughlin, J.F. (1989) The nature and significance of pseudotachylite from the Nason Terrane, North Cascades Mountains, Washington. Journal of Structural Geology, 11, 907-917.

Magloughlin, J.F. (1993) A Nason Terrane trilogy; I, Nature and significance of pseudotachylite; II, Summary of the structural and tectonic history; III,

FEBRERO 20-GEOCIENCIAS-VOL 12-2 ULTIMA VERSION.prn
D:\GEOCIENCIAS V-12-2-DIC 2008\GEOCIENCIAS-VOL 12-2 DIC.vp
viernes, 20 de febrero de 2009 13:09:19

Composite 133 lpi at 45 degrees

Major and trace element geochemistry and strontium and neodymium isotope geochemistry of the Chiwaukum Schist, amphibolite, and meta-tonalite gneiss of the Nason Terrane. University of Minnesota, Doctor of Philosophy thesis, 325 p.

McGroder, M.F. (1991) Reconciliation of two-sided thrusting, burial metamorphism, and diachronous uplift in the Cascades of Washington and British Columbia. Geological Society of America Bulletin, 103, 189-209.

Mehnert, K.R. (1968) Migmatites and the Origin of Granitic Rocks, Elsevier, Amsterdam. 393 p.

Mehnert, K.R., Busch, W., and Schneider, G. (1973) Initial melting at grain boundaries of quartz and feldspar in gneisses and granulites. Neues Jahrbuch für Mineralogie, 4, 165-183.

Miller, R.B., Haugerud, R.A., Murphy, F., and Nicholson, L.S. (1994) Tectonostratigraphic framework of the northeastern Cascades. In Lasmanis, R., and Cheney Eric, S., eds., Regional geology of Washington State Bulletin, 73-92.

Miller, R.B. and Paterson, S.R. (2001) Influence of lithological heterogeneity, mechanical anisotropy, and magmatism on the rheology of an arc, North Cascades, Washington. Tectonophysics, 342, 351-370.

Powell, R. and Holland, T.J.B. (1988) An internally consistent dataset with uncertainties and correlations; 3, Applications to geobarometry, worked examples and a computer program. Journal of Metamorphic Geology, 6, 173-204.

Powell, R. and Holland, T. (1994) Optimal geothermometry and geobarometry. American Mineralogist, 79, 120-133.

Powell, R., Holland, T., and Worley, B. (1998) Calculating phase diagrams involving solid solutions via non-linear equations, with examples using THERMOCALC. Journal of Metamorphic Geology, 16, 577-588.

Rosenberg, E.A. (1961) Geology and petrology of the Northern Wenatchee Ridge area, Northern Cascades, Washington. University of Washington, Master Science thesis, 97 p.

Sawyer, E.W. (1999) Criteria for the recognition of partial melting. Physics and Chemistry of the Earth (A), 24, 260-279.

Spear, F.S. (1988) The Gibbs method and Duhem's theorem; the quantitative relationships among *P*, *T*, chemical potential, phase composition and reaction progress in igneous and metamorphic systems. Contributions to Mineralogy and Petrology, 99, 249-256.

Spear, F.S. and Selverstone, J. (1983) Quantitative P-T paths from zoned minerals: Theory and tectonic applications. Contributions to Mineralogy and Petrology, 83, 348-357.

St-Onge, M.R. (1987) Zoned poikiloblastic garnets: P-T paths and syn-metamorphic uplift through 30 km of structural depth, Wopmay Orogen, Canada. Journal of Petrology, 28, 1-22.

Stowell, H.H., Taylor, D.L., Tinkham, D.K., Goldberg, S.A., and Ouderkirk, K.A. (2001) Contact metamorphic *P-T-t* paths from Sm-Nd garnet ages, phase equilibria modeling, and thermobarometry. Journal of Metamorphic Geology, 19, 645-660.

Stowell, H.H., and Tinkham, D. (2003) Integration of Phase Equilibria Modeling and Garnet Sm-Nd Chronology for Construction of *P-T-t* Paths: Examples from the Cordilleran Coast Plutonic Complex, USA. In D. Vance, W. Müller, and I.M. Villa, Eds., Geochronology: Linking the Isotopic Record with Petrology and Textures, 220, 119-145. The Geological Society, London.

Stowell H.H., Bulman G.R., Zuluaga C.A., Tinkham D.K., Miller R.B., & Stein, E., 2007. Mid-crustal Late Cretaceous metamorphism in the Nason terrane, Cascades crystalline core, Washington, USA: Implications for tectonic models. Memoir 200: 4-D Framework of Continental Crust: Vol. 200, p. 211-232.

Tabor, R.W., Frizzell, A., Jr., Whetten, J.T., Waitt, R.B., Jr., Swanson, D.A., Byerly, G.R., Booth,

FEBRERO 20-GEOCIENCIAS-VOL 12-2 ULTIMA VERSION.prn
D:\GEOCIENCIAS V-12-2-DIC 2008\GEOCIENCIAS-VOL 12-2 DIC.vp
viernes, 20 de febrero de 2009 13:09:19

Composite 133 lpi at 45 degrees

D.B., Hetherington, M.J., and Zartman, R.E. (1987) Geologic map of the Chelan 30' by 60' Quadrangle, Washington: U. S. Geological Survey, Reston, VA, United States.

Tabor, R.W., Frizzell, A., Jr., Booth, D.B., Waitt, R.B., Whetten, J.T., and Zartman, R.E. (1993) Geologic map of the Skykomish River 30- by 60-minute Quadrangle, Washington: U. S. Geological Survey, Reston, VA, United States.

Taylor, N.W. (1994) Structural geology of the Çhiwaukum Schist in the Mount Stuart region, central Cascades, Washington. University of Southern California, Master Science thesis, 154 p.

Tinkham, D.K., Zuluaga, C.A., and Stowell, H.H. (2001) Metapelite phase equilibria modeling in MnNCKFMASH: The effect of variable Al_2O_3 and MgO/(MgO+FeO) on mineral stability. Geological Materials Research, 3, 1-42.

Tinkham, D.K. (2002) MnNCKFMASH metapelite phase equilibria, garnet activity modeling, and garnet Sm-Nd chronology: applications to the Waterville Formation, Maine, and south-central Nason terrane, Washington. University of Alabama. Doctor of Philosophy thesis, 324 p.

Valley, P.M., Whitney, D.L., Paterson, S.R., Miller, R.B., and Alsleben, H. (2003) Metamorphism of the deepest exposed arc rocks in the Cretaceous to Paleogene Cascades belt, Washington: evidence for large-scale vertical motion in a continental arc. Journal of Metamorphic Geology, 21, 203-220.

Vance, D. and Mahar, E. (1998) Pressure-temperature paths from *P-T* pseudosections and zoned garnets; potential, limitations and examples from the Zanskar Himalaya, NW India. Contributions to Mineralogy and Petrology, 132, 225-245.

Van Diver, B.B. (1967) Contemporaneous faulting-metamorphism in Wenatchee Ridge area, Northern Cascades, Washington. American Journal of Science, 265, 132-150.

Walker, N.W. and Brown, E.H. (1991) Is the southeast Coast Plutonic Complex the consequence of accretion of the Insular Superterrane? evidence from U-Pb zircon geochronometry in the Northern Washington Cascades. Geology, 19, 714-717.

White, R.W., Powell, R., and Holland, T.J.B. (2001) Calculation of partial melting equilibria in the system Na_2O-CaO-K_2O-FeO-MgO-Al_2O_3-SiO_2-H_2O (NCKFMASH). Journal of Metamorphic Geology, 19, 139-153.

Whitney, D.L. (1992a) High-pressure metamorphism in the Western Cordillera of North America; an example from the Skagit Gneiss, North Cascades. Journal of Metamorphic Geology, 10, 71-85.

Whitney, D.L. (1992b) Origin of CO_2-rich fluid inclusions in leucosomes from the Skagit migmatites, North Cascades, Washington, USA. Journal of Metamorphic Geology, 10, 715-725.

Whitney, D.L. and McGroder, M.F. (1989) Cretaceous crust section through the proposed Insular-Intermontane suture, North Cascades, Washington. Geology, 17, 555-558.

Whitney, D.L., Miller, R.B., and Paterson, S.R. (1999) *P-T-t* evidence for mechanisms of vertical tectonic motion in a contractional orogen; north-western US and Canadian Cordillera. Journal of Metamorphic Geology, 17, 75-90.

Zuluaga, C.A., 2004. Thermodynamic modeling applied to metamorphic processes in migmatites: an example from the Nason Ridge Migmatitic Gneiss (Cascades Core, WA). 177 p. Ph.D. thesis, University of Alabama, Tuscaloosa.

Zuluaga, C.A., Stowell, H.H., Tinkham, D.K., 2005. The effect of zoned garnet on metapelite pseudosection topology and calculated metamorphic *P-T* paths. American Mineralogist 90, 1619-1628.

FEBRERO 20-GEOCIENCIAS-VOL 12-2 ULTIMA VERSION.prn
D:\GEOCIENCIAS V-12-2-DIC 2008\GEOCIENCIAS-VOL 12-2 DIC.vp
viernes, 20 de febrero de 2009 13:09:19